



Effets de la pression sur les Plasmas d'Entrée Atmosphérique Planétaire et sur les Plasmas induits par Laser

Arnaud BULTEL

CORIA, UMR CNRS 6614, Normandie Université, 76801 Saint-Etienne du Rouvray cedex, FRANCE

arnaud.bultel@coria.fr



Sommaire

1. Plasmas d'Entrée Atmosphérique Planétaire

Contexte

Physique de l'Entrée Atmosphérique Planétaire

Modèles Collisionnels-Radiatifs ↔ Influence de la Pression

2. Plasmas induits par Laser

Contexte

Physique des Plasmas induits par Laser

Expériences ↔ Résultats de Modèles Collisionnels-Radiatifs

Effets de la Pression

Sommaire

1. Plasmas d'Entrée Atmosphérique Planétaire

Contexte

Physique de l'Entrée Atmosphérique Planétaire

Modèles Collisionnels-Radiatifs ↔ Influence de la Pression

2. Plasmas induits par Laser

Contexte

Physique des Plasmas induits par Laser

Expériences ↔ Résultats de Modèles Collisionnels-Radiatifs

Effets de la Pression

Earth Natural Entries...



Police patrol at Edmonton, Canada

(November, 20th 2008, 23:30 UTC)



Chelyabinsk, Russia

(February, 15th 2013, 03:20 UTC)

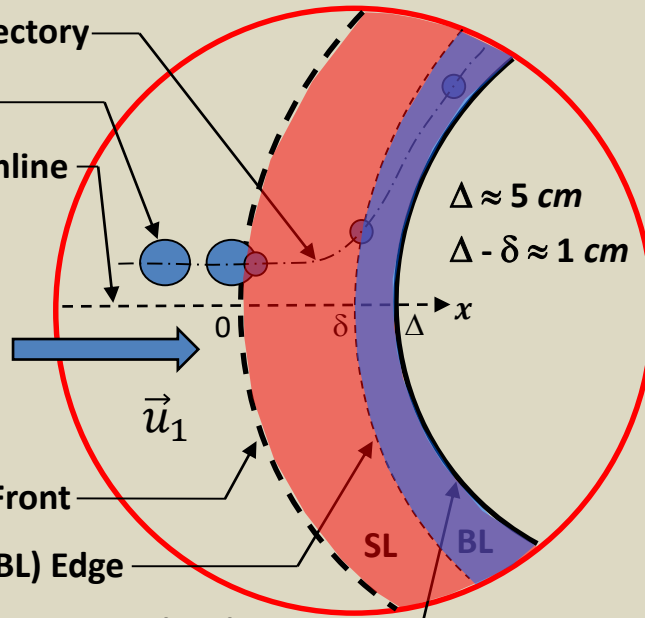
Simplification along the stagnation streamline

$(u_1 \text{ 5 to } 15 \text{ km s}^{-1})$

Fluid particle trajectory

Fluid particle

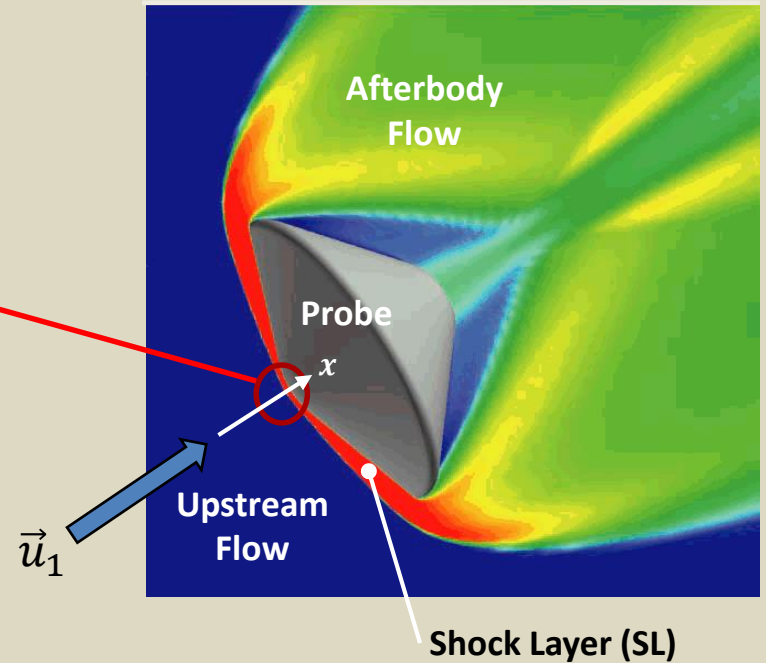
Stagnation streamline



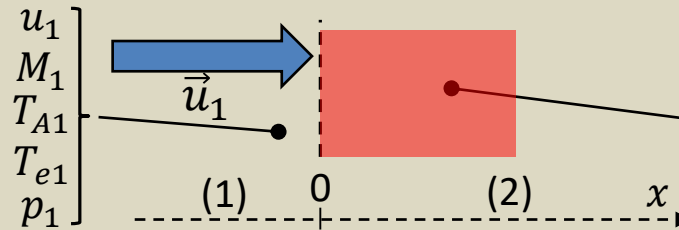
Detached Shock Front

Boundary Layer (BL) Edge

Thermal Protection System (TPS)



Post-shock relaxation



$$\begin{bmatrix} u_2(x) \\ M_2(x) \\ T_{A2}(x) \\ T_{e2}(x) \\ p_2(x) \end{bmatrix} \quad u_2(0), M_2(0), T_{A2}(0), T_{e2}(x), p_2(0)$$

Rankine-Hugoniot equations
RH1D codes

Post-shock relaxation

Species **Heavies at T_A**
Electrons at T_e

Balance equations (no diffusion)

- 1. Species balance
- 2. Momentum balance
- 3. Energy balance

$$\frac{dy_{X_m}}{dx} = \frac{m_{X_m} [\dot{X}_m]}{\rho u}$$

$$\frac{d(p + \rho u^2)}{dx} = 0$$

Heavies (atoms, molecules, ions)

Electrons

$$\frac{d}{dx} \left[\frac{e_A}{\rho} + \frac{p_A}{\rho} + \frac{\rho_A}{\rho} \frac{u^2}{2} \right] = \frac{-Q_{A \rightarrow e} - \epsilon_{Rad} - Q_{A-RR}}{\rho u}$$

$$\frac{d}{dx} \left[\frac{e_e}{\rho} + \frac{p_e}{\rho} + \frac{\rho_e}{\rho} \frac{u^2}{2} \right] = \frac{Q_{A \rightarrow e} - \epsilon_{RR} + Q_{A-RR}}{\rho u}$$

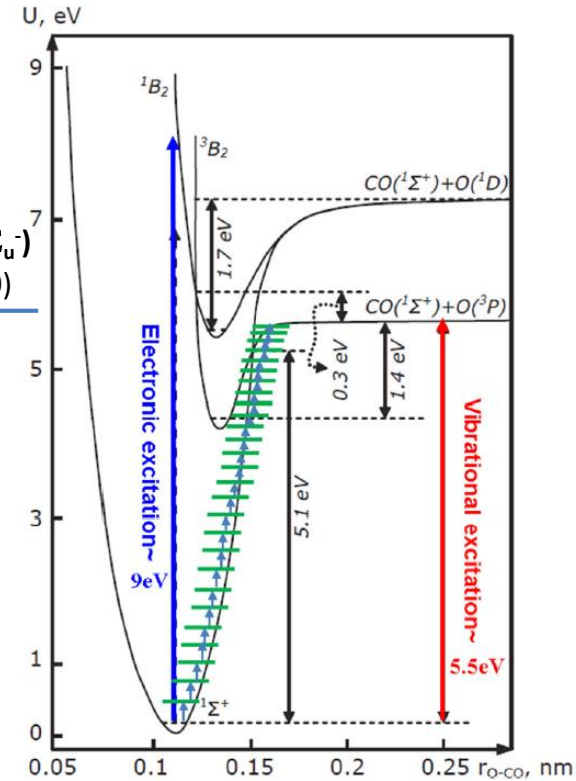
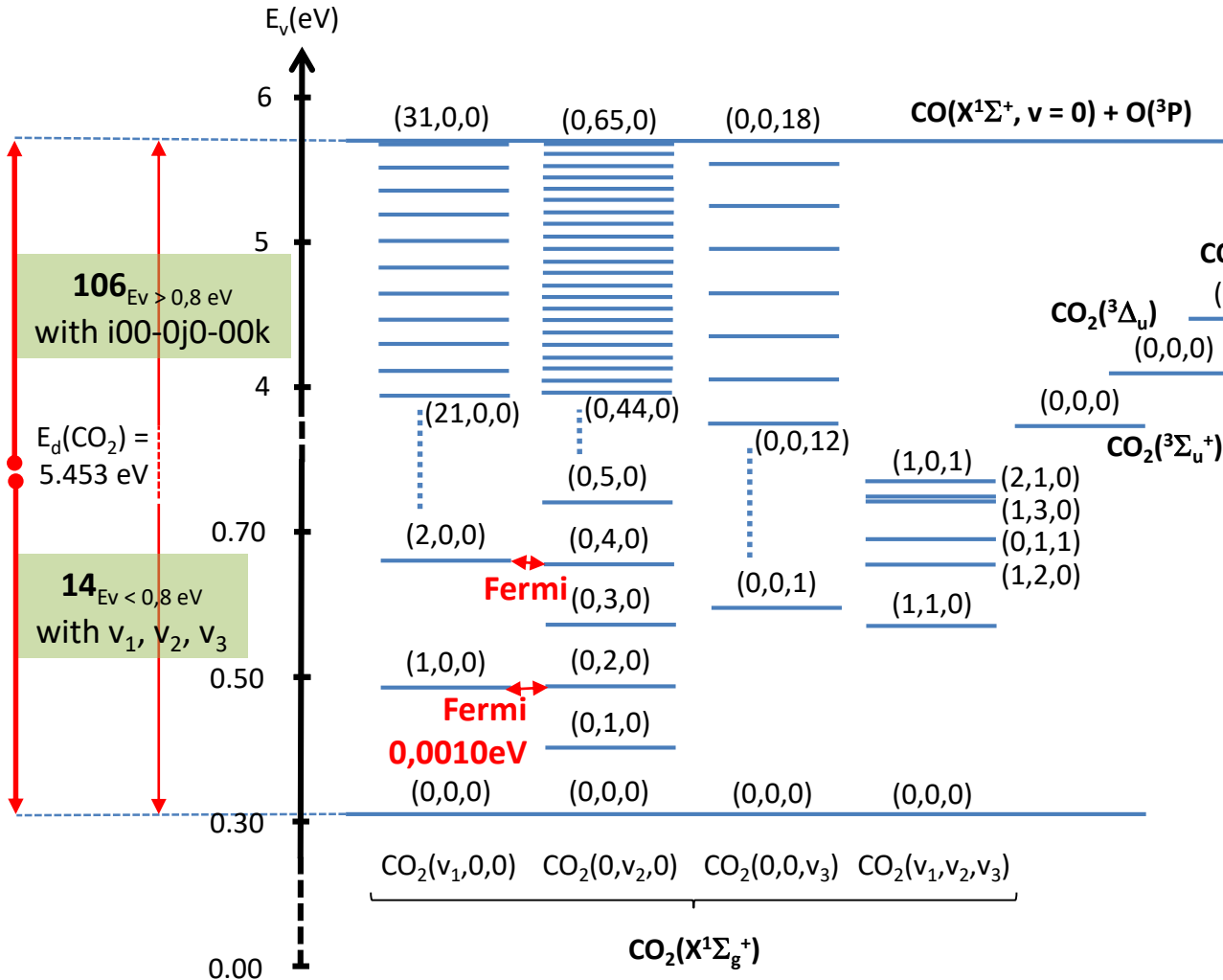
Collisional-radiative source terms



Type	21 species 1600 states		
Molecules	CO₂	$X^1\Sigma_g^+(14_{Ev < 0,8 eV}$ with v_1, v_2, v_3 , and $106_{Ev > 0,8 eV}$ with i00-0j0-00k) $^3\Sigma_u^+, ^3\Delta_u, ^3\Sigma_u^-$	
	N₂	$X^1\Sigma_g^+(v = 0 \rightarrow 67)$ $A^3\Sigma_u^+, B^3\Pi_g, W^3\Delta_u, B'^3\Sigma_u^-, a'^1\Sigma_u^-, a^1\Pi_g, w^1\Delta_u, G^3\Delta_g, C^3\Pi_u, E^3\Sigma_g^+$	
	O ₂	$X^3\Sigma_g^-(v = 0 \rightarrow 46)$ $a^1\Delta_g, b^1\Sigma_g^+, c^1\Sigma_g^-, A'^3\Delta_u, A^3\Sigma_u^+, B^3\Sigma_u^-, f^1\Sigma_u^+$	
	C ₂	$X^1\Sigma_g^+(v = 0 \rightarrow 36)$ $a^3\Pi_u, b^3\Sigma_g^-, A^1\Pi_u, c^3\Sigma_u^+, d^3\Pi_g, C^1\Pi_g, e^3\Pi_g, D^1\Sigma_u^+$	
	NO	$X^2\Pi(v = 0 \rightarrow 53)$ $a^4\Pi, A^2\Sigma^+, B^2\Pi, b^4\Sigma^-, C^2\Pi, D^2\Sigma^+, B'^2\Delta, E^2\Sigma^+, F^2\Delta$	
	CO	$X^1\Sigma^+(v = 0 \rightarrow 76)$ $a^3\Pi, a'^3\Sigma^+, d^3\Delta, e^3\Sigma^-, A^1\Pi, I^1\Sigma^-, D^1\Delta^-, b^3\Sigma^+, B^1\Sigma^+$	
	CN	$X^2\Sigma^+(v = 0 \rightarrow 41)$ $A^2\Pi, B^2\Sigma^+, D^2\Pi, E^2\Sigma^+, F^2\Delta$	
	Molecular ions	N ₂ ⁺	$X^2\Sigma_g^+, A^2\Pi_u, B^2\Sigma_u^+, a^4\Sigma_u^+, D^2\Pi_g, C^2\Sigma_u^+$
		O ₂ ⁺	$X^2\Pi_g, a^4\Pi_u, A^2\Pi_u, B^4\Sigma_g^-$
		C ₂ ⁺	$X^4\Sigma_g^-, ^1\Pi_u, ^4\Pi_u, ^1\Sigma_g^+, ^2\Pi_u, B^4\Sigma_u^-, ^1\Sigma_u^+$
NO ⁺		$X^1\Sigma^+, a^3\Sigma^+, b^3\Pi, W^3\Delta, b'^3\Sigma^-, A'^1\Sigma^+, W^1\Delta, A^1\Pi$	
CO ⁺		$X^2\Sigma^+, A^2\Pi, B^2\Sigma^+, C^2\Delta$	
CN ⁺		$X^1\Sigma^+, a^3\Pi, ^1\Delta, c^1\Sigma^+$	
Atoms	N	$^4S^{\circ}_{3/2}, ^2D^{\circ}_{5/2}, ^2D^{\circ}_{3/2}, ^2P^{\circ}_{1/2}, \dots\dots\dots(252 \text{ states})$	
	O	$^3P_2, ^3P_1, ^3P_0, ^1D_2, \dots\dots\dots(127 \text{ states})$	
	C	$^3P_0, ^3P_1, ^3P_2, ^1D_2, \dots\dots\dots(265 \text{ states})$	
	Ar	$^1S_0, ^2[3/2]^{\circ}_2, ^2[3/2]^{\circ}_1, ^2[1/2]^{\circ}_0, \dots\dots(379 \text{ states})$	
Atomic ions	N ⁺	$^3P_0, ^3P_1, ^3P_2, ^1D_2, \dots\dots\dots(9 \text{ states})$	
	O ⁺	$^4S^{\circ}_{3/2}, ^2D^{\circ}_{5/2}, ^2D^{\circ}_{3/2}, ^2P^{\circ}_{3/2}, \dots\dots\dots(8 \text{ states})$	
	C ⁺	$^2P^{\circ}_{1/2}, ^2P^{\circ}_{3/2}, ^4P_{1/2}, ^4P_{3/2}, \dots\dots\dots(8 \text{ states})$	
	Ar ⁺	$^2P^{\circ}_{3/2}, ^2P^{\circ}_{1/2}, ^2S_{1/2}, ^4D_{7/2}, \dots\dots\dots(7 \text{ states})$	

Vibrational states of CO₂

MARS atmosphere 96 % CO₂ 2 % N₂ 2 % Ar



Q. Huang *et al.*, J. Phys. D: Appl. Phys. **50** 294001 2017

CoRaM-MARS

Elementary processes $T_e \neq T_A$

- Collisional processes** (e- and h-) vibrational processes
 (e- and h-) electronic excitation
 Excitation transfer
 Dissociation
 Ionisation
 Charge exchange
 Dissociative recombination
- Radiative processes** Main molecular systems
 Main atomic transitions
- « Dual » processes** Radiative recombination
 Dielectronic recombination

→ ~ 1 000 000 elementary processes

Rate coefficients and Einstein coefficients

Rate coefficients

Forward rate coefficients

$$k_i(T_{A,e}) = \sqrt{\frac{8 k_B T_{A,e}}{\pi \mu}} \int_{x_0}^{+\infty} x e^{-x} \sigma_i(x) dx$$

with $\sigma_i(x)$ the cross section and $x = \frac{\varepsilon}{k_B T_{A,e}}$

the reduced collision energy

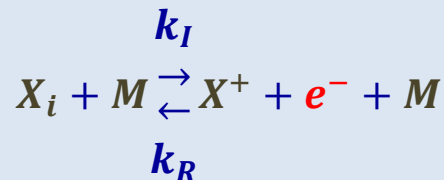
Backward rate coefficients from

Detailed Balance

Einstein coefficients

NIST database

Ionisation/recombination by heavy particle impact under thermal non equilibrium



J. Annaloro, P. Teulet, A. Bultel *et al.*

Eur. Phys. J. D. **17** (2017) 342

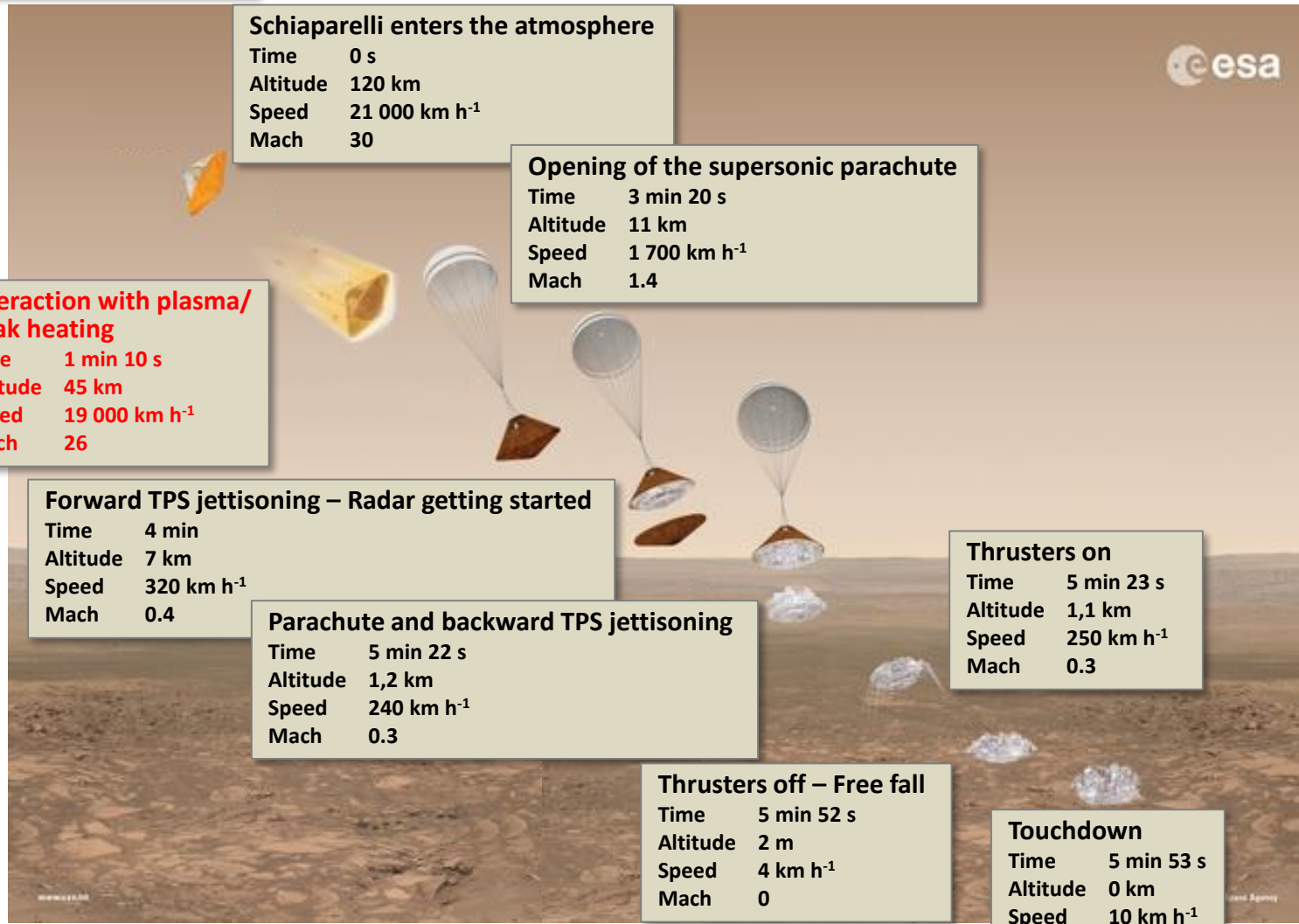
k_I depends on T_A

k_R depends on T_A and T_e

$$\frac{k_I}{k_R} = \frac{g_+ g_e}{g_i} \left(\frac{2\pi m_e k_B T_e}{h^2} \right)^{3/2} e^{-\frac{E_i^{ioni}}{k_B T_A}}$$

EXOMARS mission

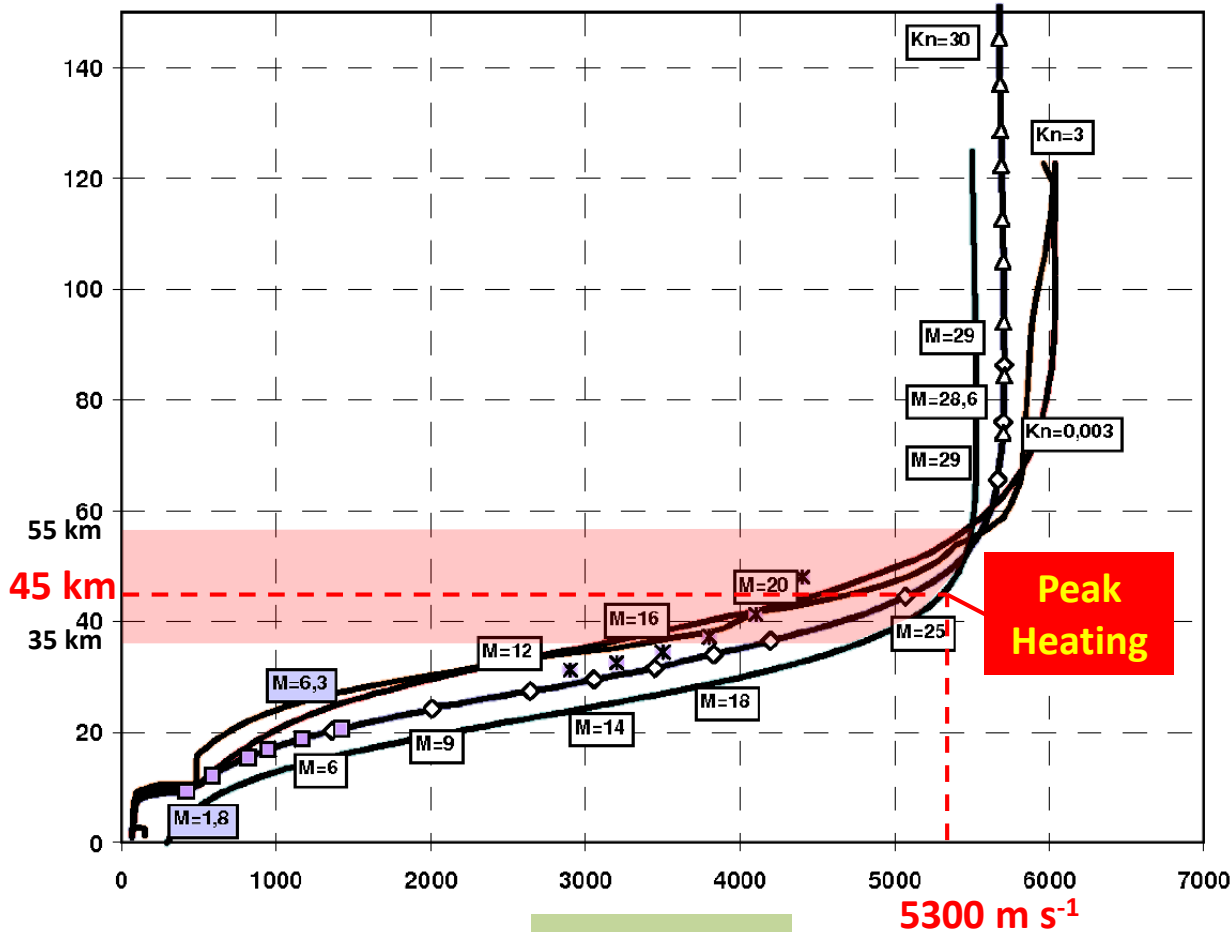
October, 19th 2016



EXOMARS mission

October, 19th 2016

Altitude (km)



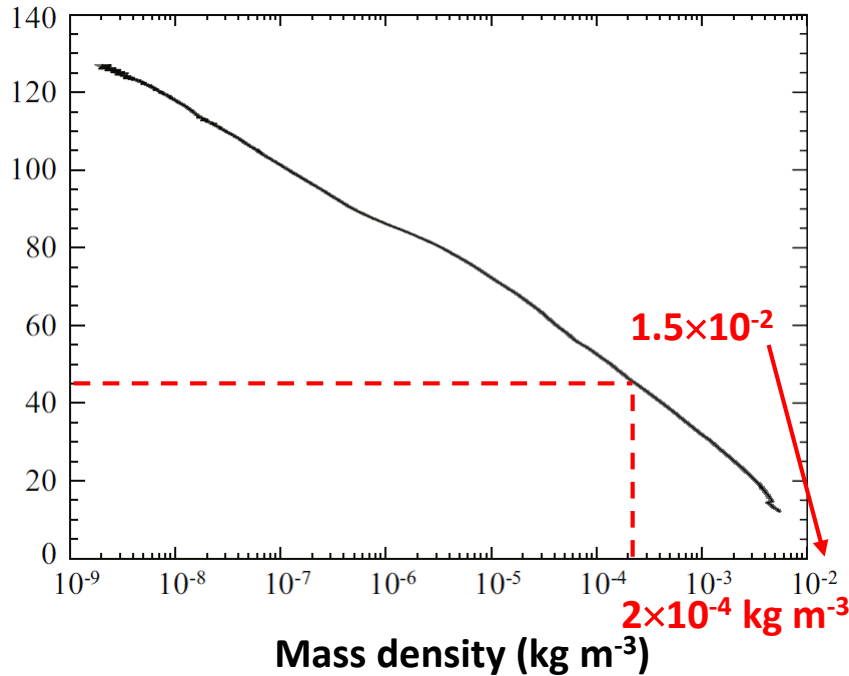
- Reference TRajjectory
- Shallow Entry - Dust Storm Season
- Steep Entry - Cold Atmosphere
- ◇ Anchor Points (Hot Hypersonic)
- △ DSMC - Anchor Points
- Cold Hypersonic - Supersonic Anchor Points
- MER Trajectory
- * Viking Trajectory

Speed (m s⁻¹)

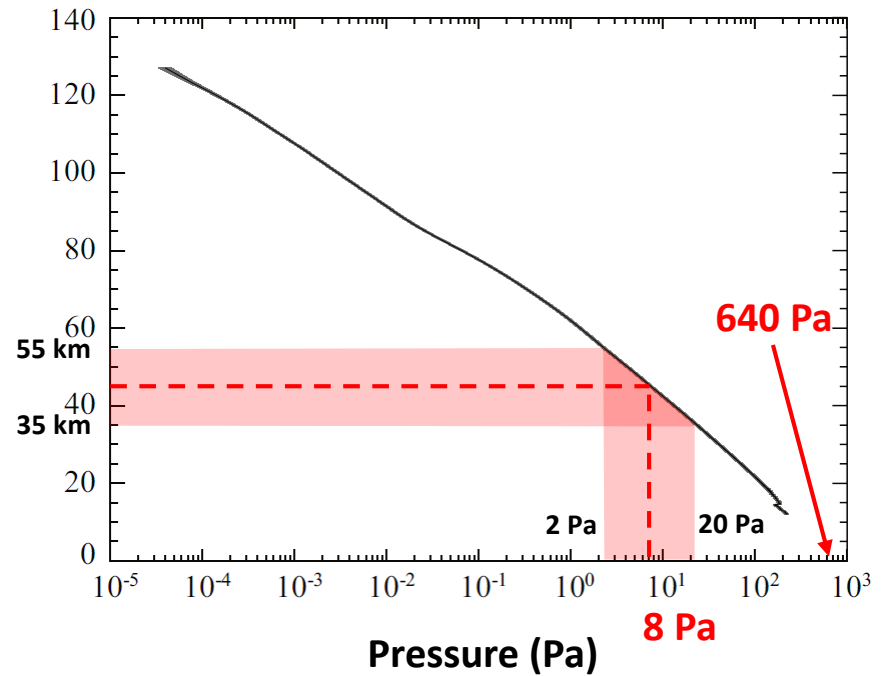
P. Tran et al.
ESA SP-692 (2011)

EXOMARS mission
October, 19th 2016

Altitude (km)



Altitude (km)



C. Holstein-Rathlou *et al.* Planet. Space Science **120** (2016) 15-23

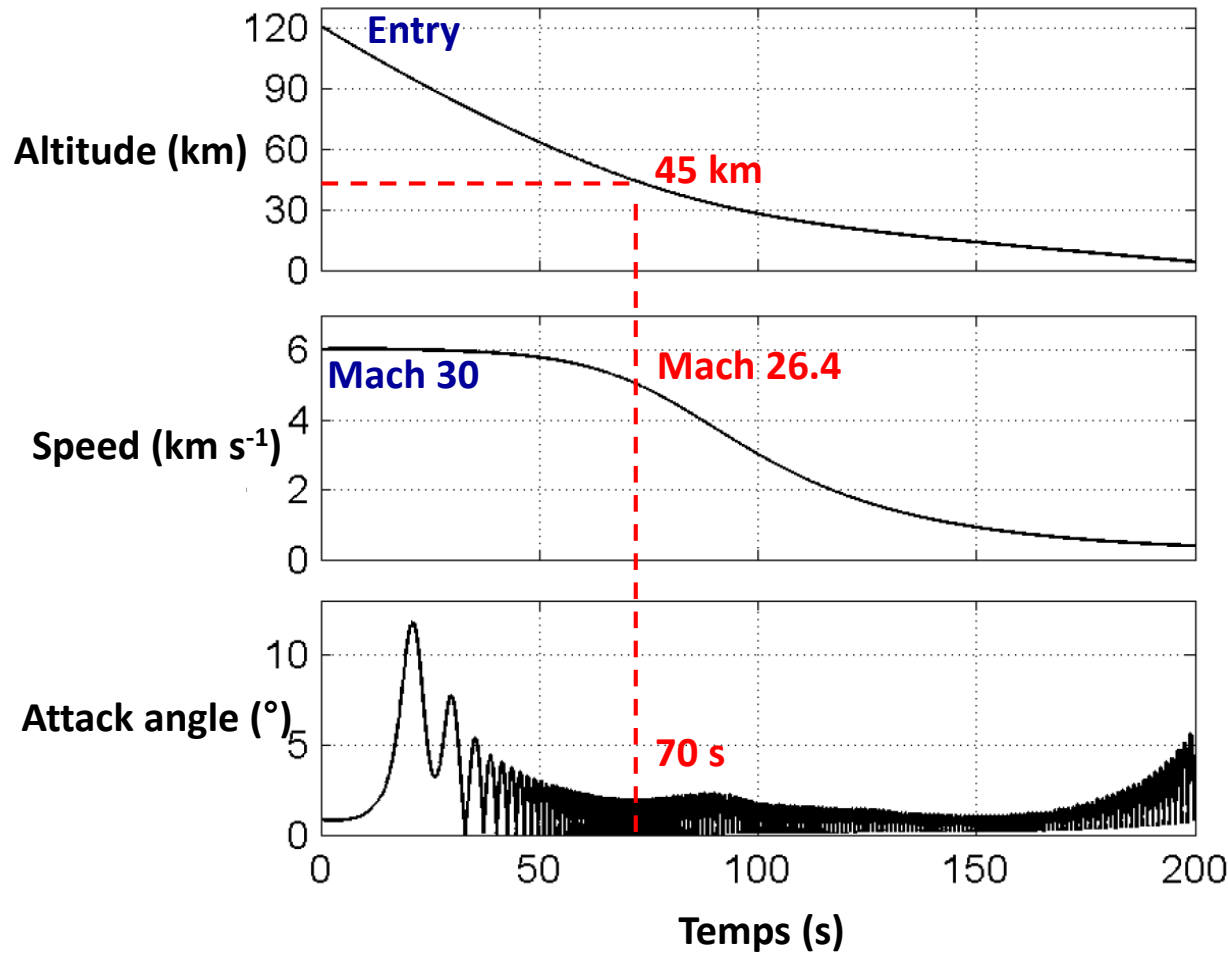
Chemical composition of the Martian atmosphere

CO₂	95.97 %	O₂	0.146 %	CH₂O	130×10^{-7} %
Ar	1.93 %	CO	0.0557 %	O₃	30×10^{-7} %
N₂	1.89 %	H₂O	0.03 %	CH₄	10.5×10^{-7} %

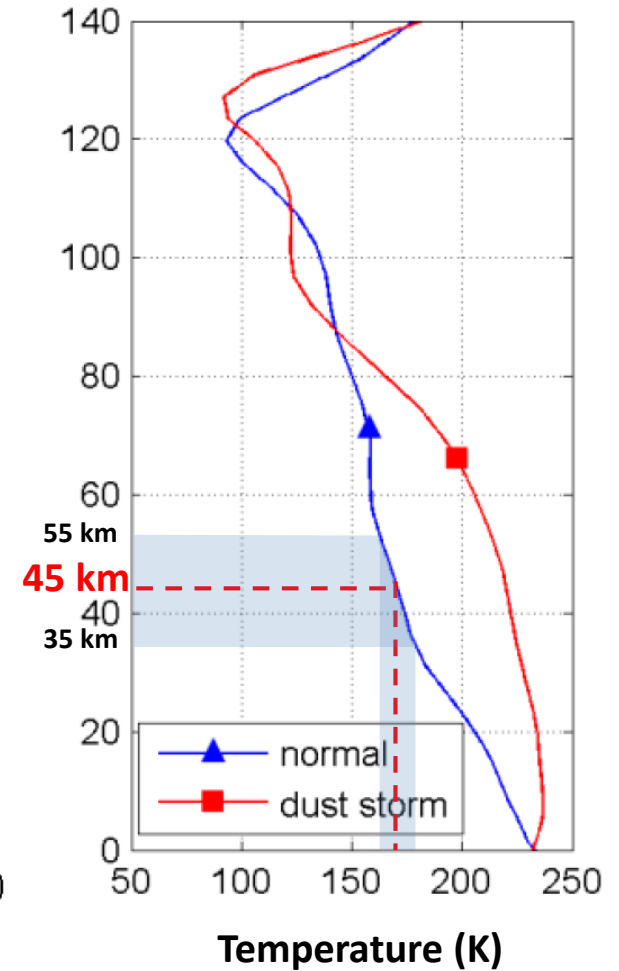
Mole fractions

EXOMARS mission

October, 19th 2016

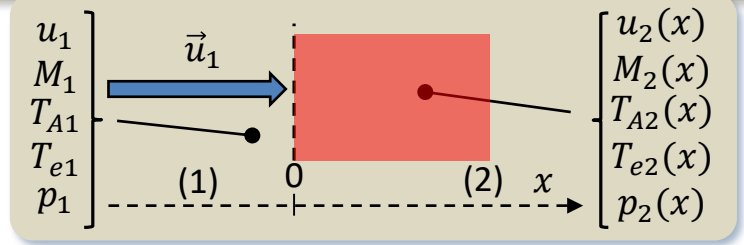


Altitude (km)



B. Van Hove *et al.* 10th IPPW 17-21 (2013)

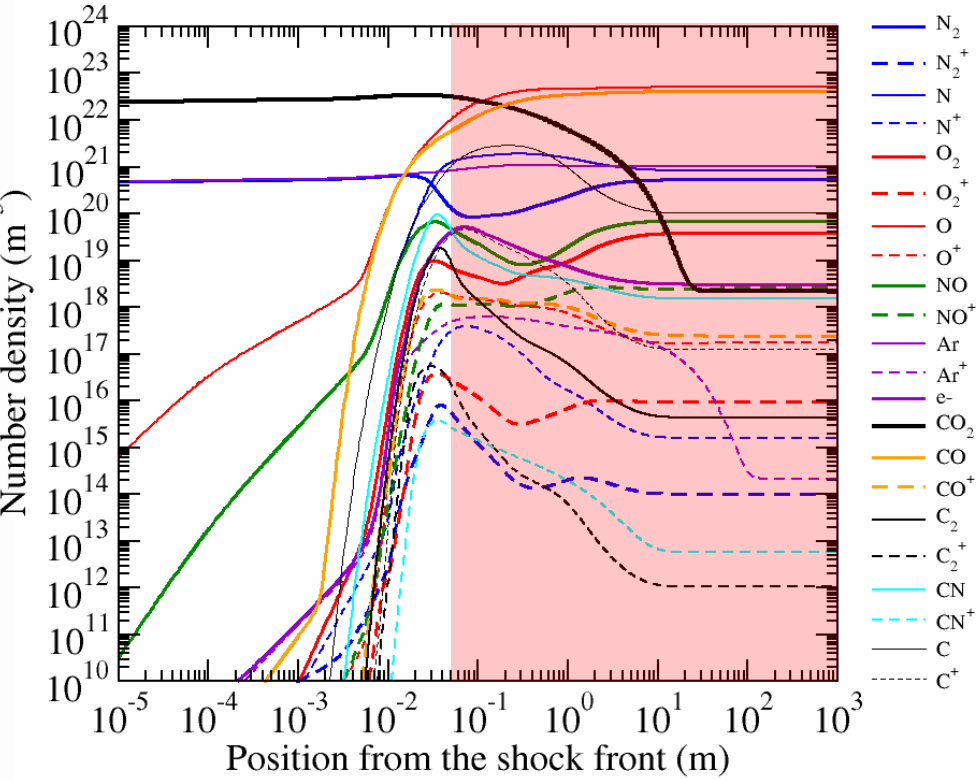
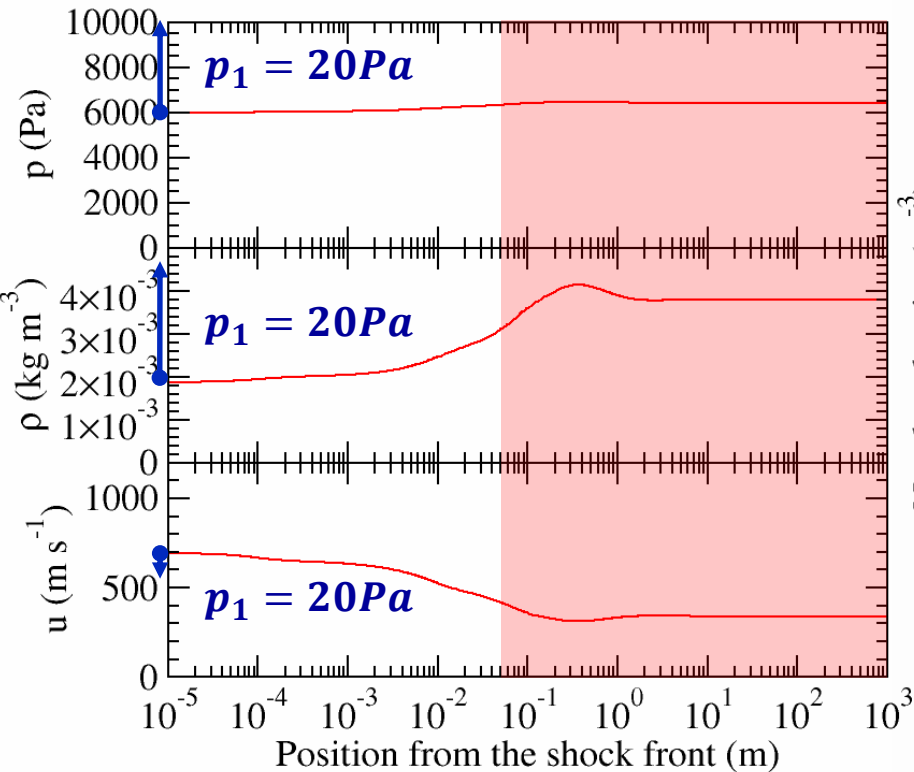
CoRaM-MARS and RH1D codes...



Aerodynamic variables

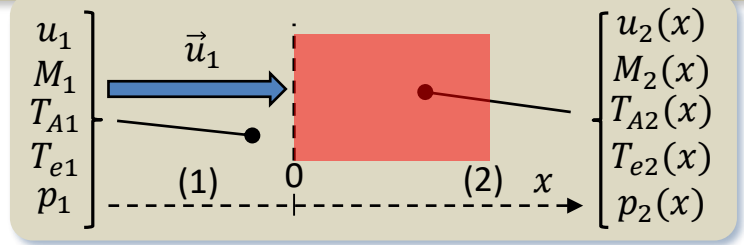
Species number densities

$p_1 = 8 Pa$

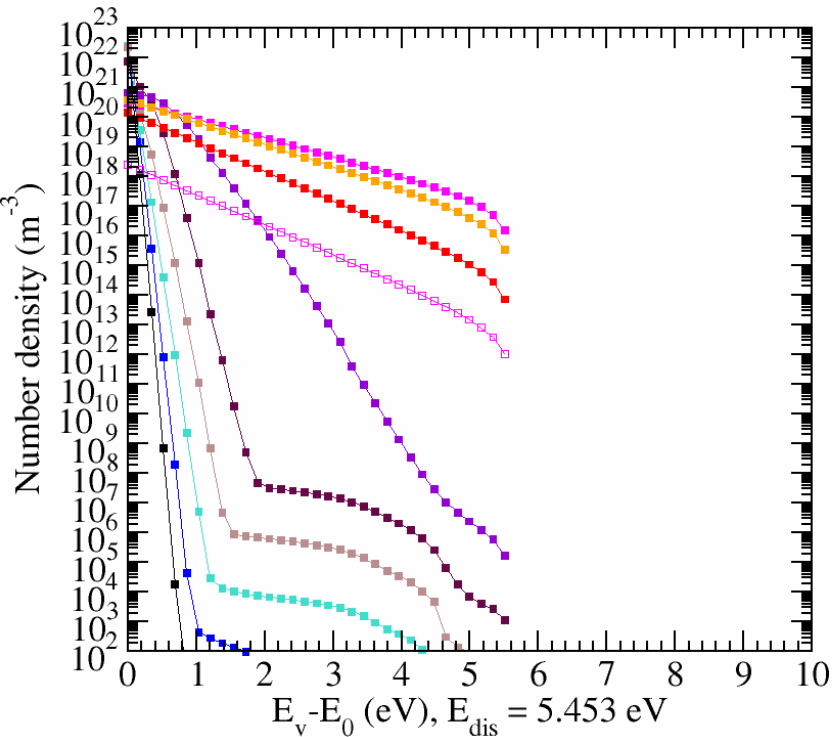


$T_{A2}(0) = 16800 K$ $T_{e2}(0) = 10900 K$

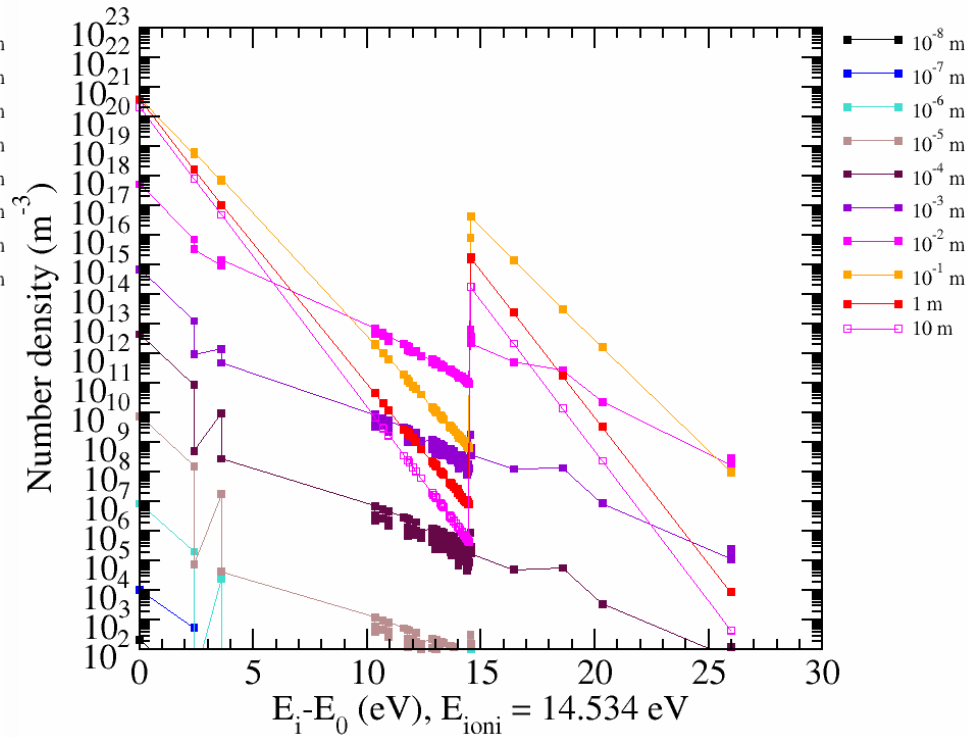
CoRaM-MARS and RH1D codes...



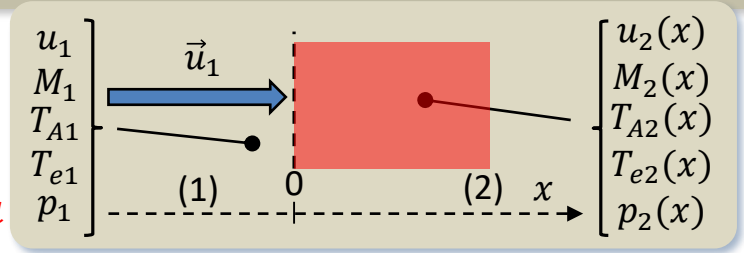
Boltzmann plots CO₂(i00)



Boltzmann plots N and N⁺



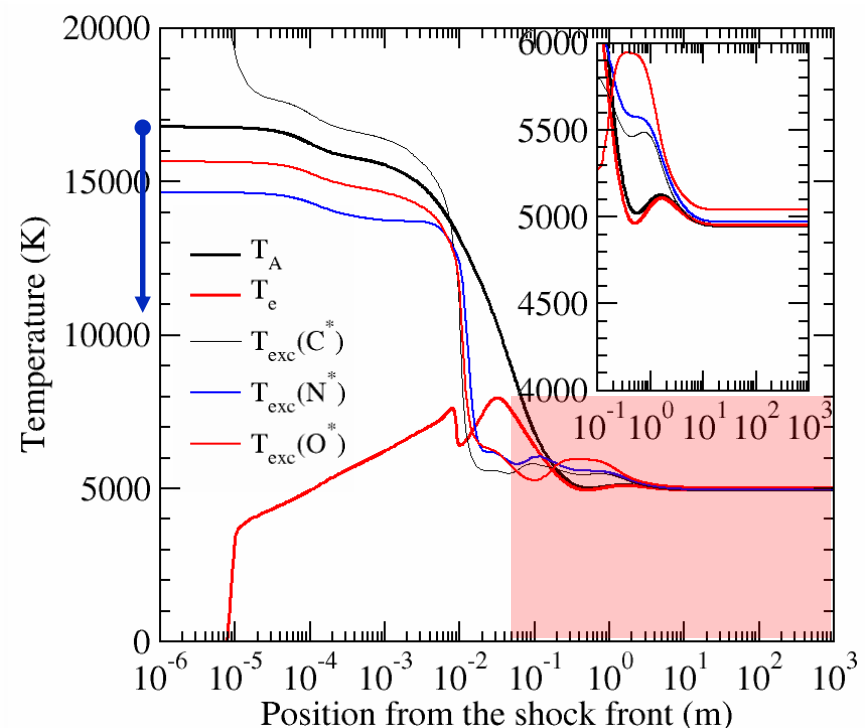
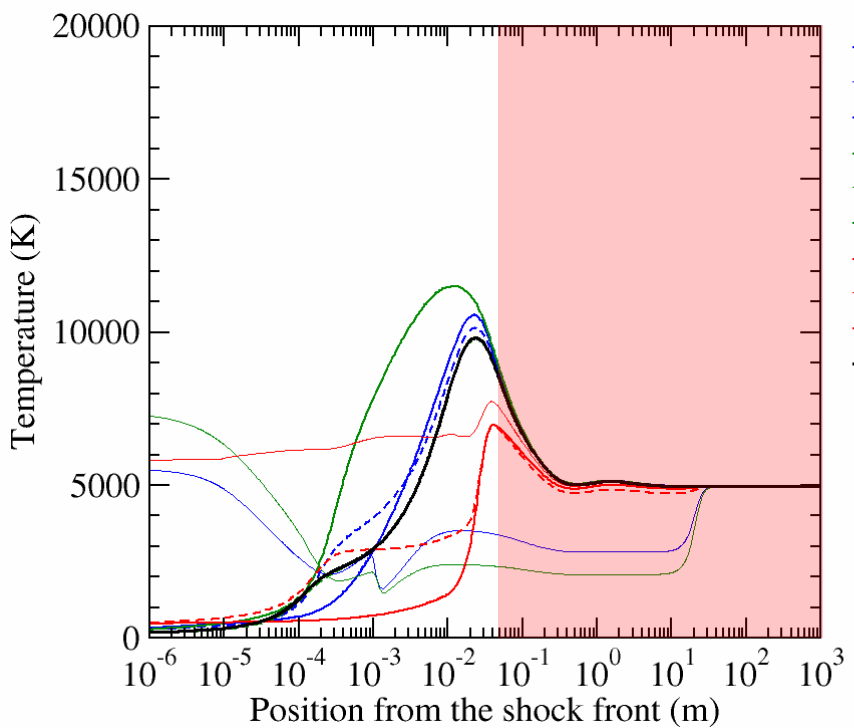
CoRaM-MARS and RH1D codes...



$p_1 = 8 \text{ Pa}$
 $p_1 = 20 \text{ Pa}$

Vibrational temperatures

Excitation temperatures



Sommaire

1. Plasmas d'Entrée Atmosphérique Planétaire

Contexte

Physique de l'Entrée Atmosphérique Planétaire

Modèles Collisionnels-Radiatifs ↔ Influence de la Pression

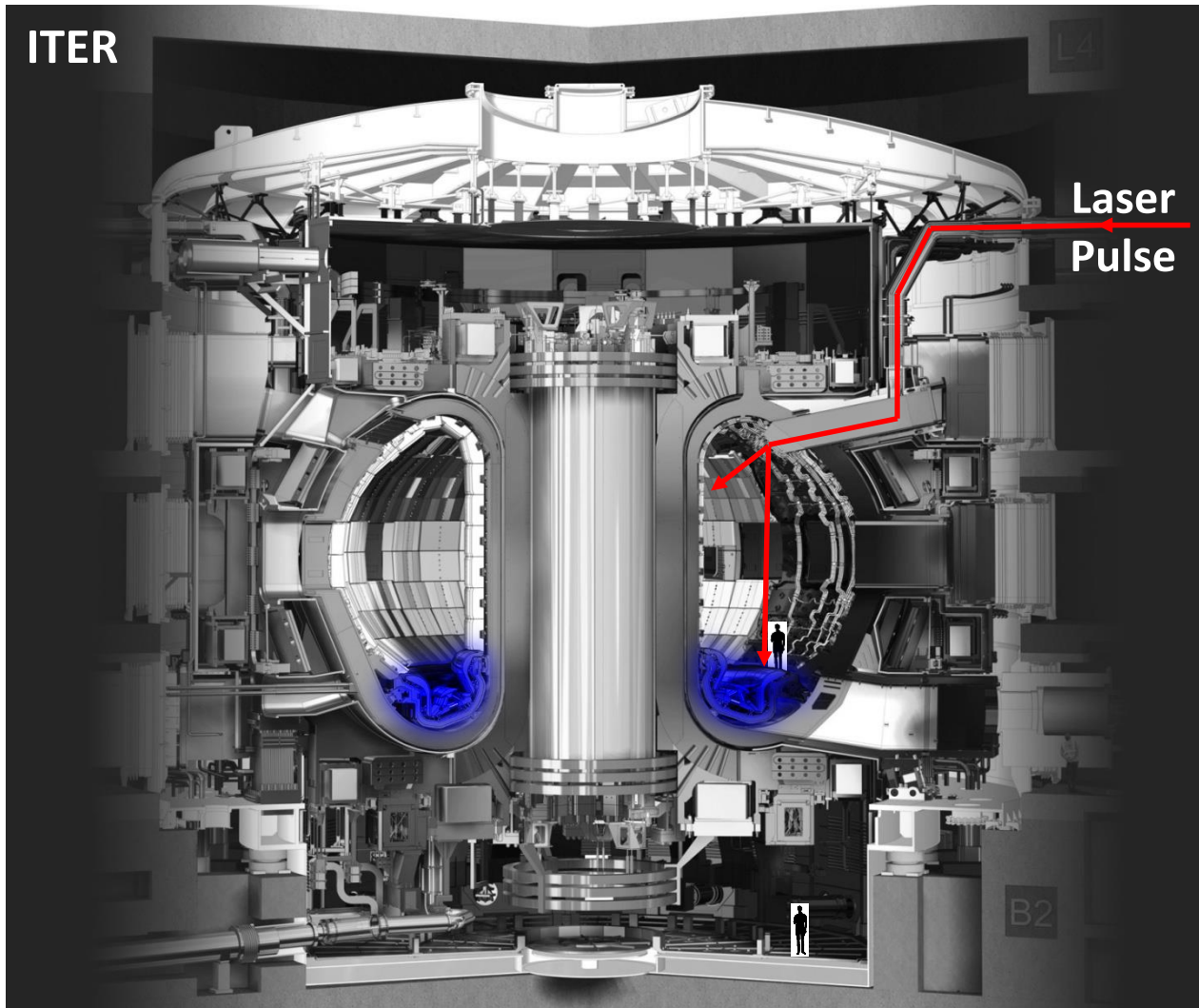
2. Plasmas induits par Laser

Contexte

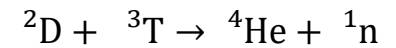
Physique des Plasmas induits par Laser

Expériences ↔ Résultats de Modèles Collisionnels-Radiatifs

Effets de la Pression



Fusion reaction



${}^3\text{T}$ radioactive

${}^3\text{T}$ has to be monitored

Implantation of ${}^3\text{T}$, ${}^2\text{D}$ (fuel) and ${}^{14}\text{N}$, ${}^{16}\text{O}$... (impurities) within the **W** divertor also in the **Be** wall

In situ measurement by
LIBS

Composition analysis by Laser-Induced Breakdown Spectroscopy – LIBS

Laser-Material interaction

Nd:YAG
(1064 nm, 30 ps)
Class IV

Lens

Shockwave

Shock layer

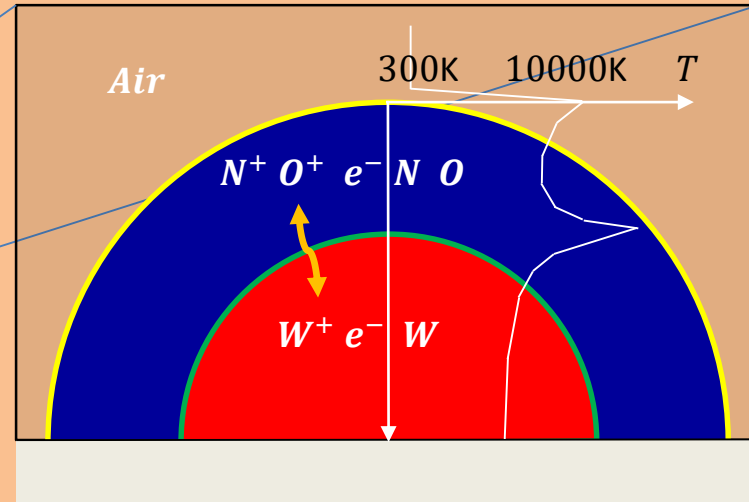
Contact surface

Ablated material

Crater

Sample

$10^{13} - 10^{14} \text{ W m}^{-2}$



Melting

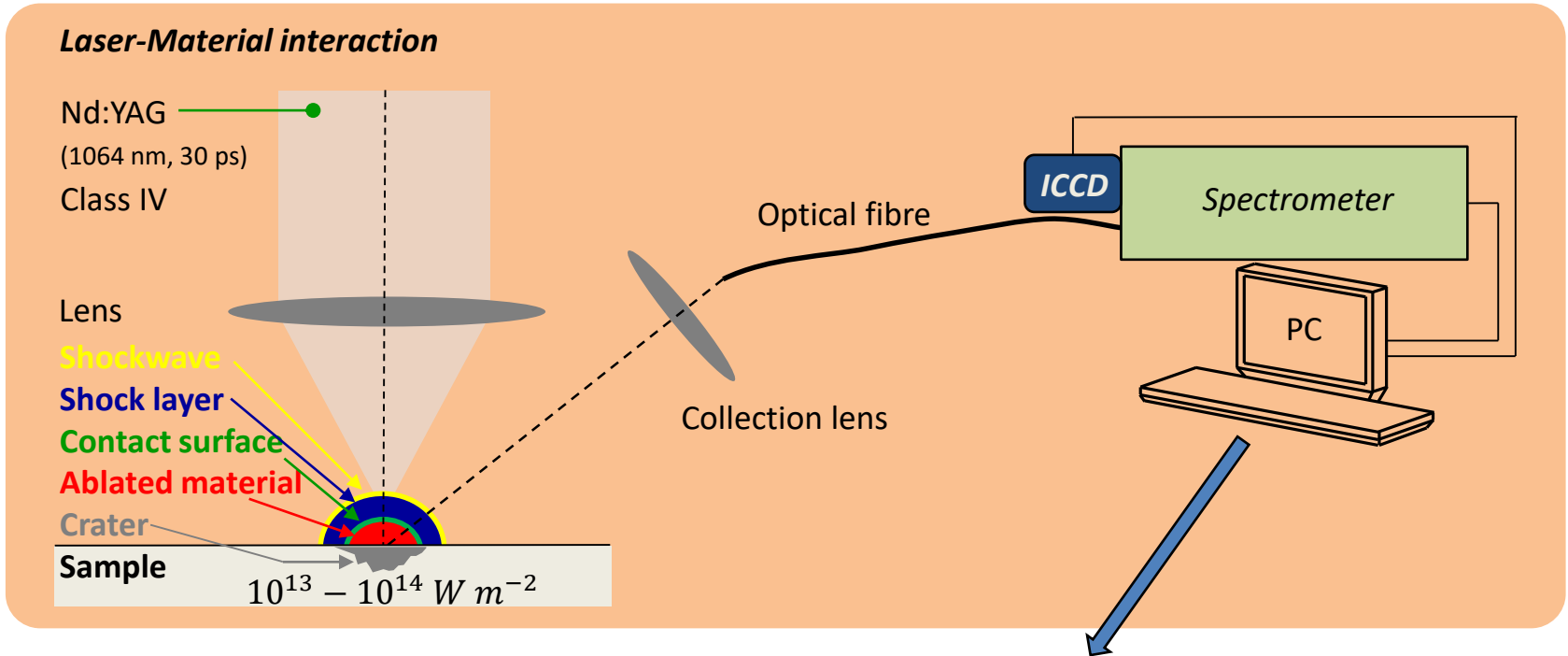
Vaporization – explosion phase

Ionization (MPI & IB)

Plasma (10^{10} Pa , 10 000 K)

Shockwave

Composition analysis by Laser-Induced Breakdown Spectroscopy – LIBS



Melting

Vaporization – explosion phase

Ionization (MPI & IB)

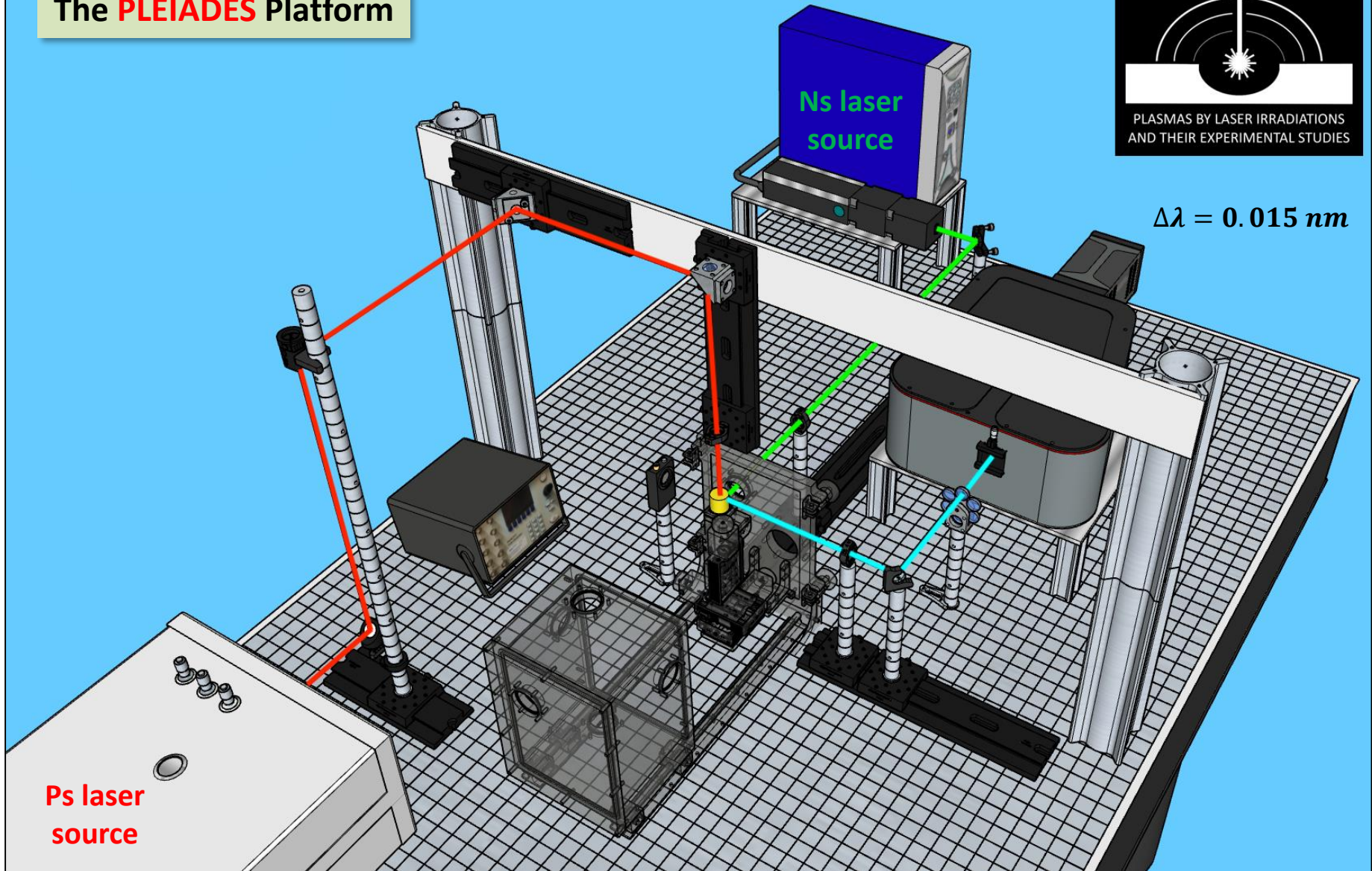
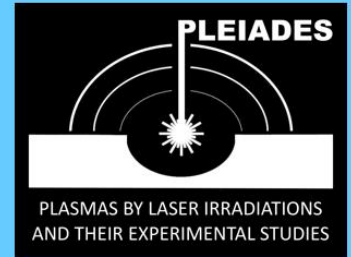
Plasma (10^{10} Pa , $10\,000 \text{ K}$)

Shockwave

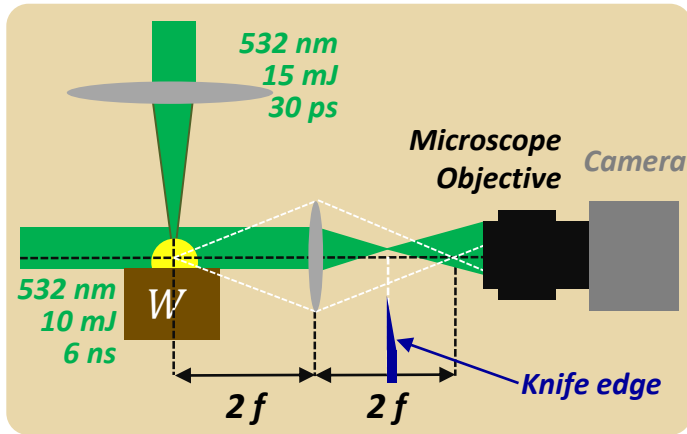
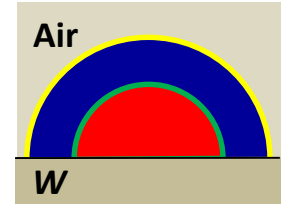
Spectroscopic analysis

- $0 < t < 100 \text{ ns}$ strong continuum
 - $t < 500 \text{ ns}$ strong departure from equilibrium
 - $t > 500 \text{ ns}$ low non equilibrium (atom. and molec. Rad.)
- ⇒ Exploitation of **Saha-Boltzmann** plots

The PLEIADES Platform

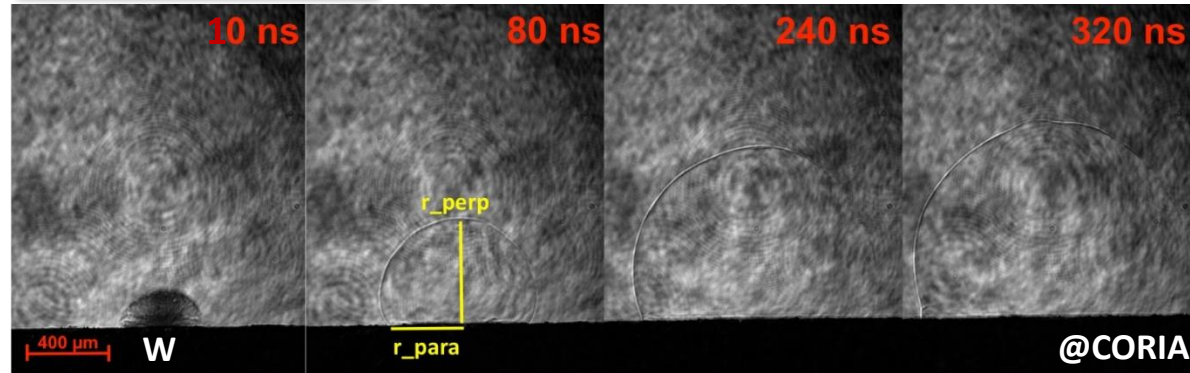


Fluid dynamics / structure



Laser shadowgraphy

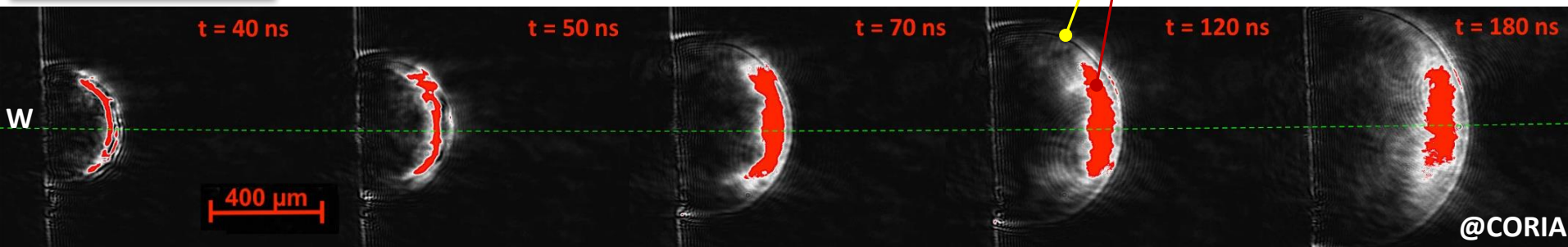
Sensitive to $\frac{\partial^2 n}{\partial z^2}$



Shockwave
Contact surface

Schlieren Imagery

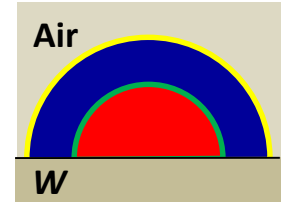
Sensitive to $\frac{\partial n}{\partial z}$



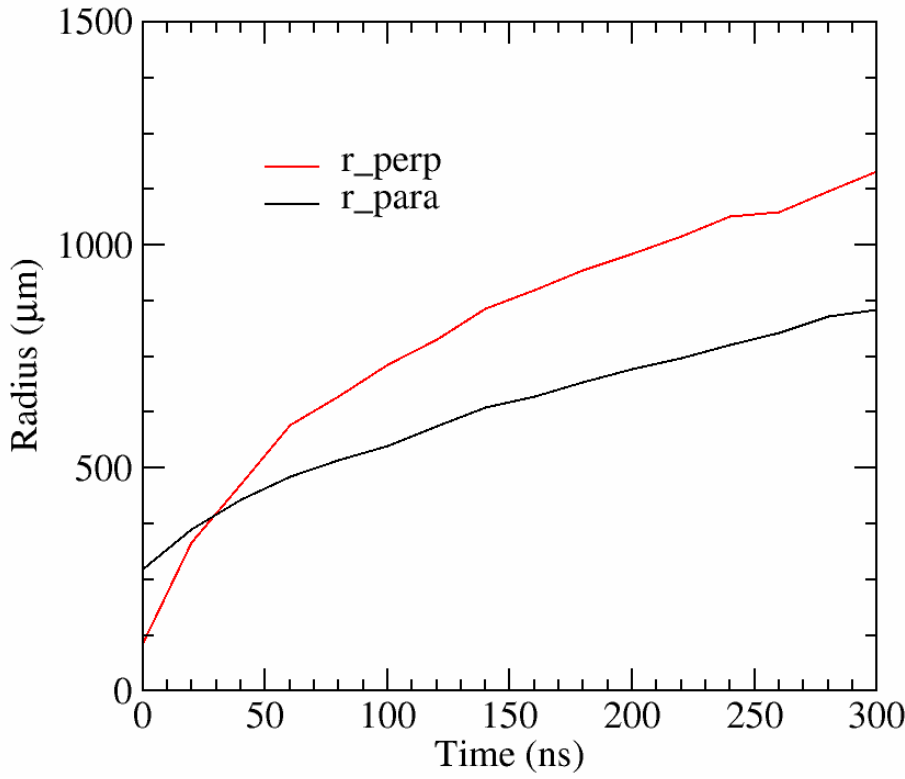
Very rapid evolution over the first 200 ns then slower evolution...

The contact surface remains close to the shock front

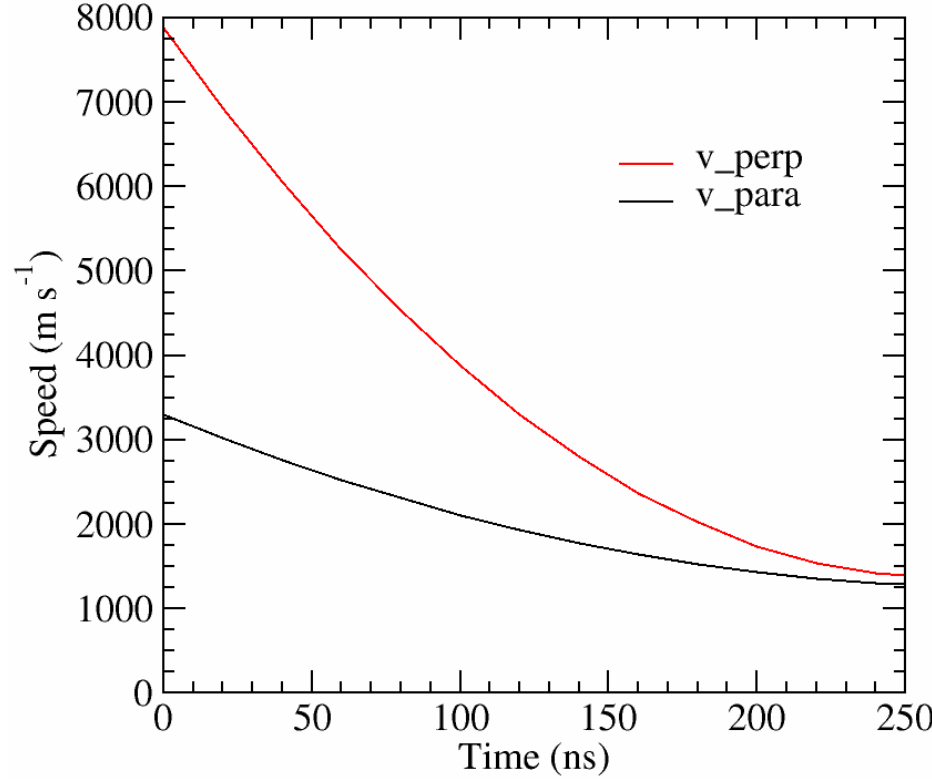
Fluid dynamics / structure



Shockwave radius



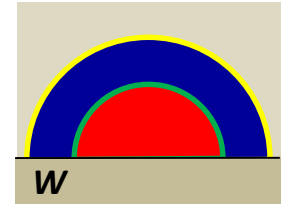
Shockwave speed



Expansion mainly perpendicular to the sample

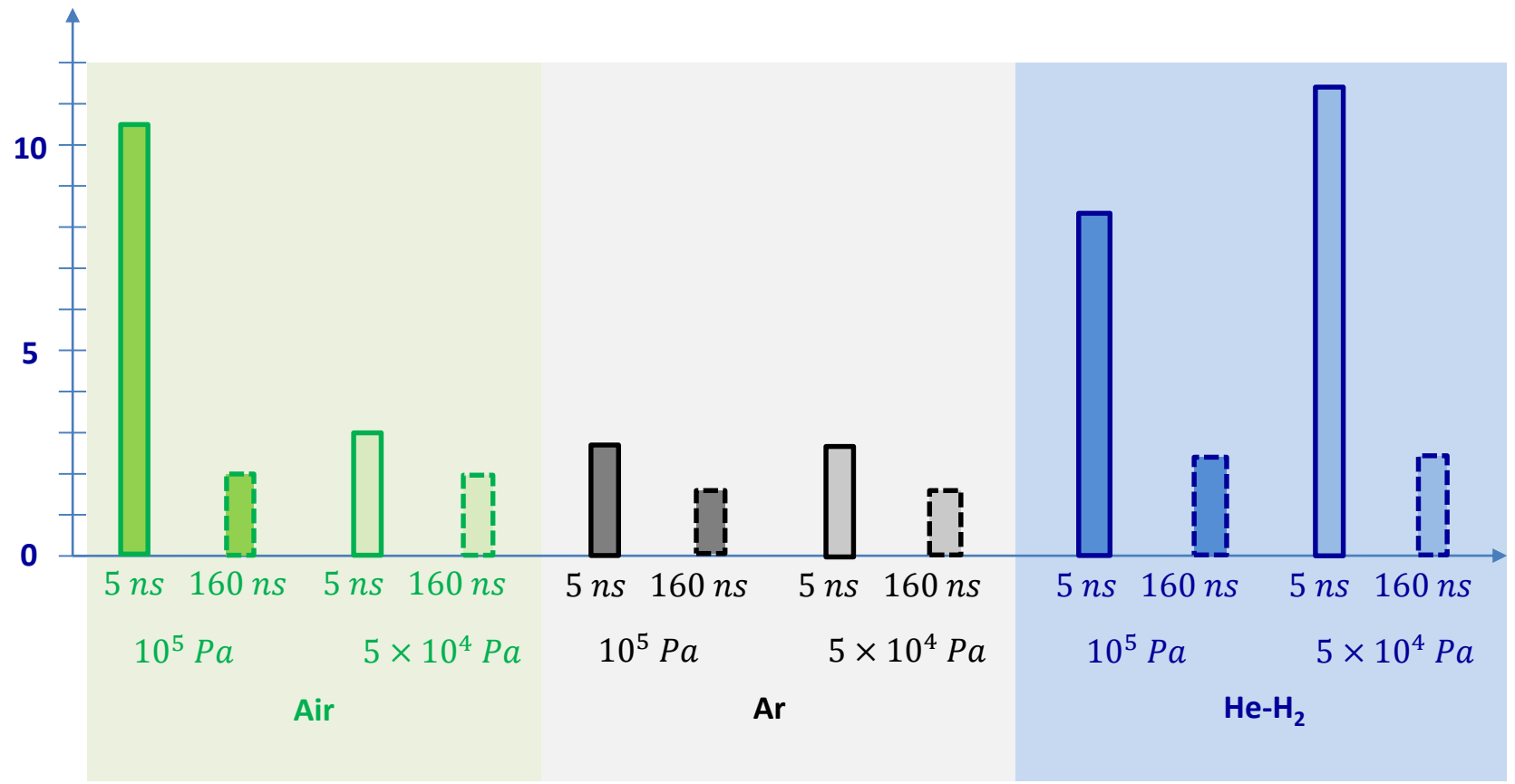
Hypersonic expansion ($\mathcal{M} \sim 25$ at the beginning...)

Fluid dynamics / structure



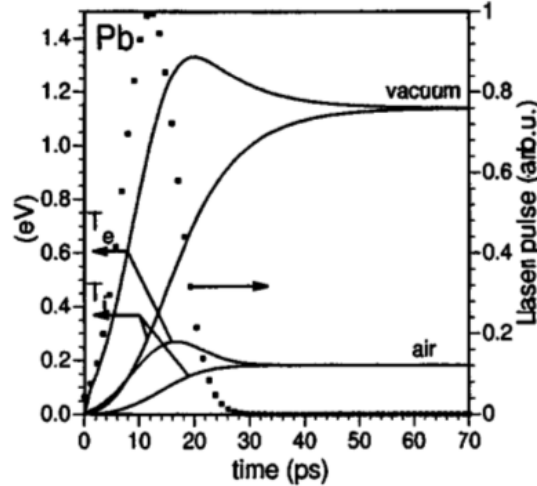
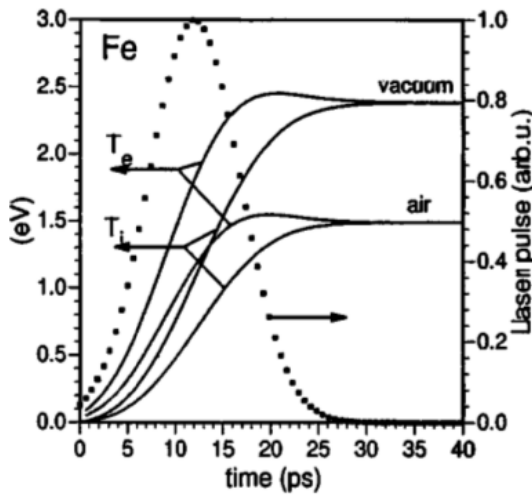
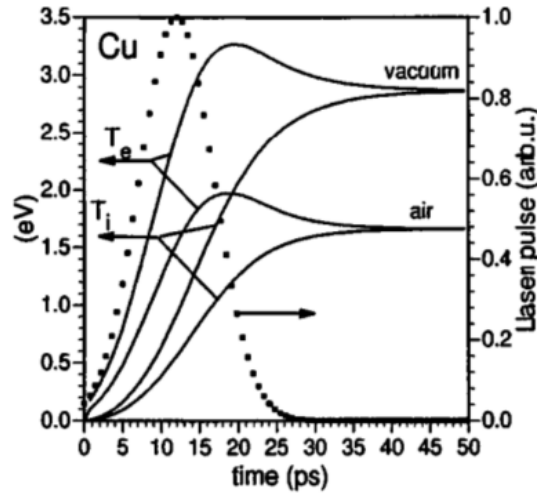
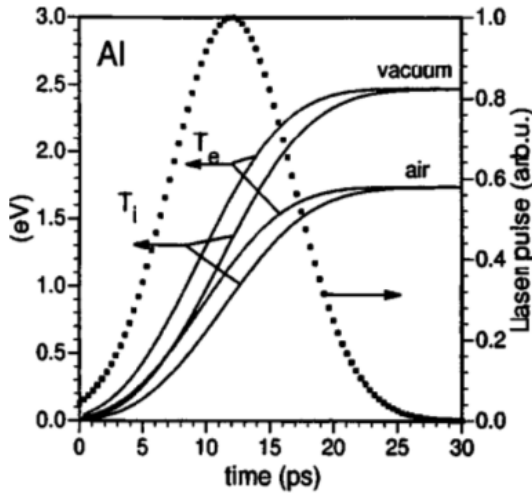
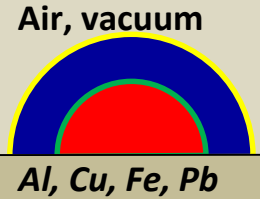
Perpendicular speed

v_{perp} ($km\ s^{-1}$)



Fluid dynamics / structure

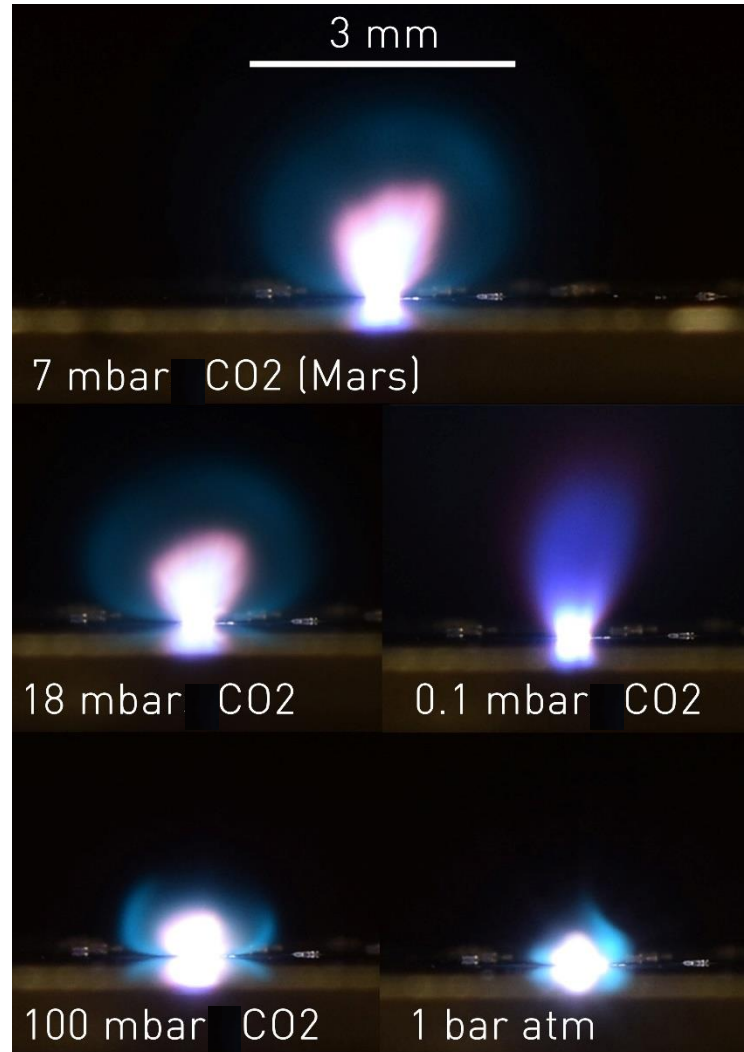
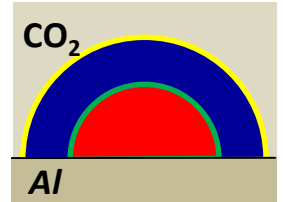
$$\tau_p \cong 10 \text{ ps}$$



T_e and T_i
in the skin layer close to
the ablation threshold

Fluid dynamics / structure

Plasma plume



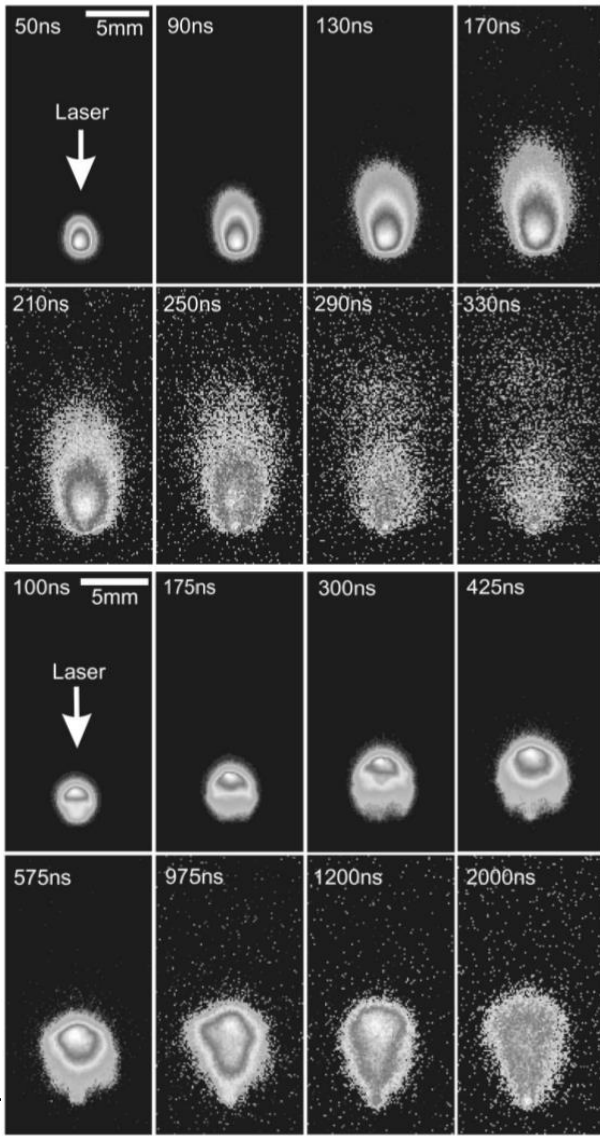
6 ns
1064 nm
40 J cm⁻²
Al (CO₂)

W. Rapin, private comm.

Fluid dynamics / structure

S.S. Harilal *et al.*
 J. Appl. Phys. **93** (2003) 2380

Plasma plume



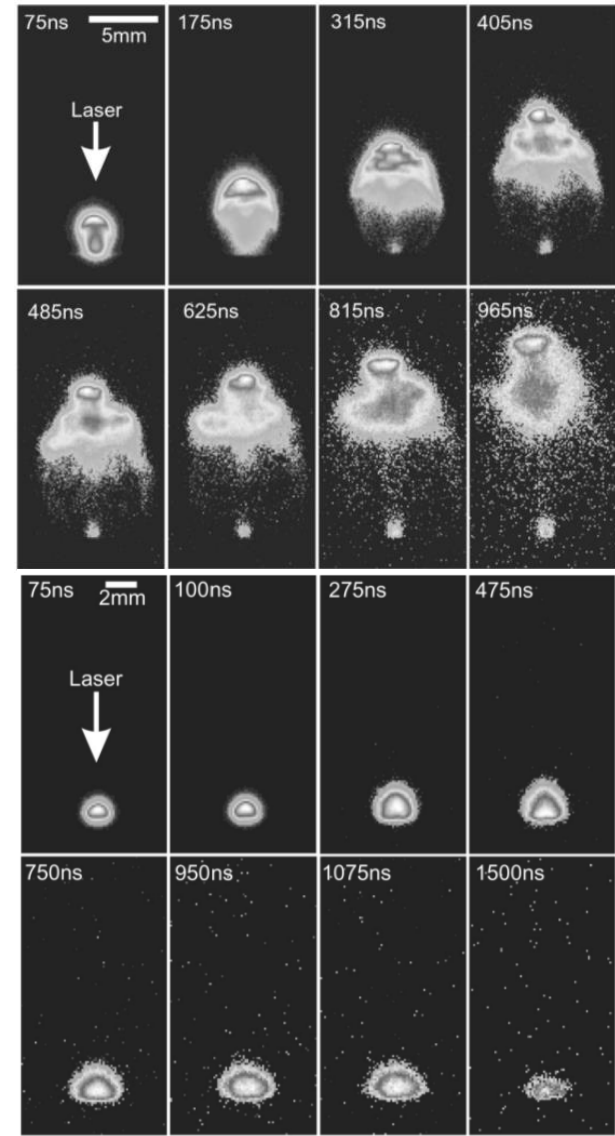
1 Pa

150 Pa

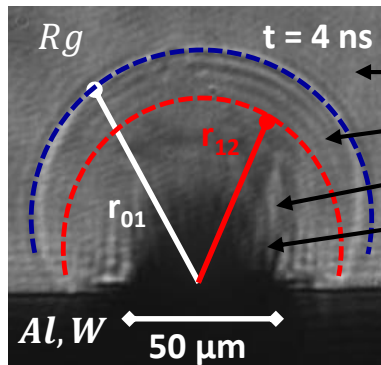
8 ns
 532 nm
 24 J cm⁻²
 Al (air)

1300 Pa

13000 Pa



Assumptions



Hypersonic hemispherical expansion

- (0) External gas (rare gas: Ne, Ar, Kr or Xe)
 - (1) Shock layer (shocked rare gas)
 - (2) Central plasma (ablated **W** ou **Al**)
- Ablated material**

- r_{01} shock front radius
- r_{12} contact surface radius
- v_{sf} shock front speed

Bi-layer model

Propagation of the shockwave
Rankine-Hugoniot assumption

Atoms and ions... at T_A
 Electrons... at T_e

Balance equations

(1) Shock layer

Mass

$$\rho_0 v_{sf} = \rho_1 [v_{sf} - u_1(r_{01})] \Leftrightarrow \frac{d\rho(\{Rg\}_j^{Z+})}{dt} = \dot{\rho}(\{Rg\}_j^{Z+}) - \frac{\rho(Rg_j^{Z+})}{\rho_1} \frac{d\rho_1}{dt}$$

Energy

$$\epsilon_0 + \frac{p_0}{\rho_0} + \frac{v_{sf}^2}{2} = \epsilon_1 + \frac{p_1}{\rho_1} + \frac{[v_{sf} - u_1(r_{01})]^2}{2}$$

Momentum

$$p_0 + \rho_0 v_{sf}^2 = p_1 + \rho_1 [v_{sf} - u_1(r_{01})]^2$$

(2) Central plasma

Mass

$$M_2 = \frac{2\pi}{3} \rho_2 r_{12}^3 \Leftrightarrow \frac{d\rho(\{Al, W\}_j^{Z+})}{dt} = \dot{\rho}(\{Al, W\}_j^{Z+}) - 3\rho(\{Al, W\}_j^{Z+}) \frac{u_2(r_{12})}{r_{12}}$$

Energy

$$E_2 = M_2 (\epsilon^{Al, W} + \epsilon_2) + E_{c,2} \Leftrightarrow \frac{dE}{dt} = \rho_0 \epsilon_0 v_{sf} 2\pi r_{01}^2 - \frac{M_2}{\rho_2} (4\pi \epsilon_{RR} + 4\pi \epsilon_{TB} + \epsilon'_{SE})$$

Momentum

$$\frac{d[u_2(r_{12})]}{dt} = \frac{8\pi}{3} \frac{r_{12}^2}{M_2} (p_2 - p_1)$$

Collisional-radiative source term

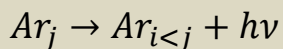
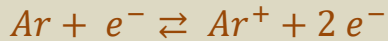
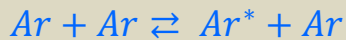
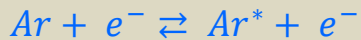
V. Morel, A. Bultel *et al.*

Spectrochim. Acta B **127** (2017) 7

Collisional-radiative models

Shock layer - Argon

Collisional-Radiative model CoRaM-RG



Exc. Elec. Impact

Exc. Elec. Impact

Ioni. Elec. Impact

Ioni. Elec. Impact

Ioni. Heavy Impact

Ioni. Heavy Impact

Penning Ioni.

Disso. Recomb.

Rad. Recomb.

Spont. Emiss.

30 000 elementary processes

Collisional Database

$$k_i(T_{A,e}) = \sqrt{\frac{8 k_B T_{A,e}}{\pi \mu}} \int_{x_0}^{+\infty} x e^{-x} \sigma_i(x) dx \text{ with}$$

• $\sigma_i(x)$ collisional cross section and

• $x = \frac{\varepsilon}{k_B T_{A,e}}$ reduced collision energy

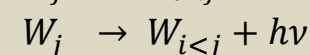
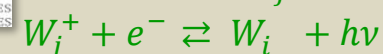
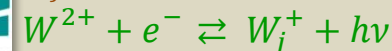
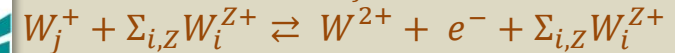
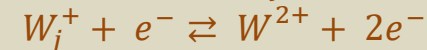
Backward rate coefficient deduced from the

Detailed Balance



Central plasma - Tungsten

Collisional-Radiative model CoRaM-W



Thermal Bremsstrahlung

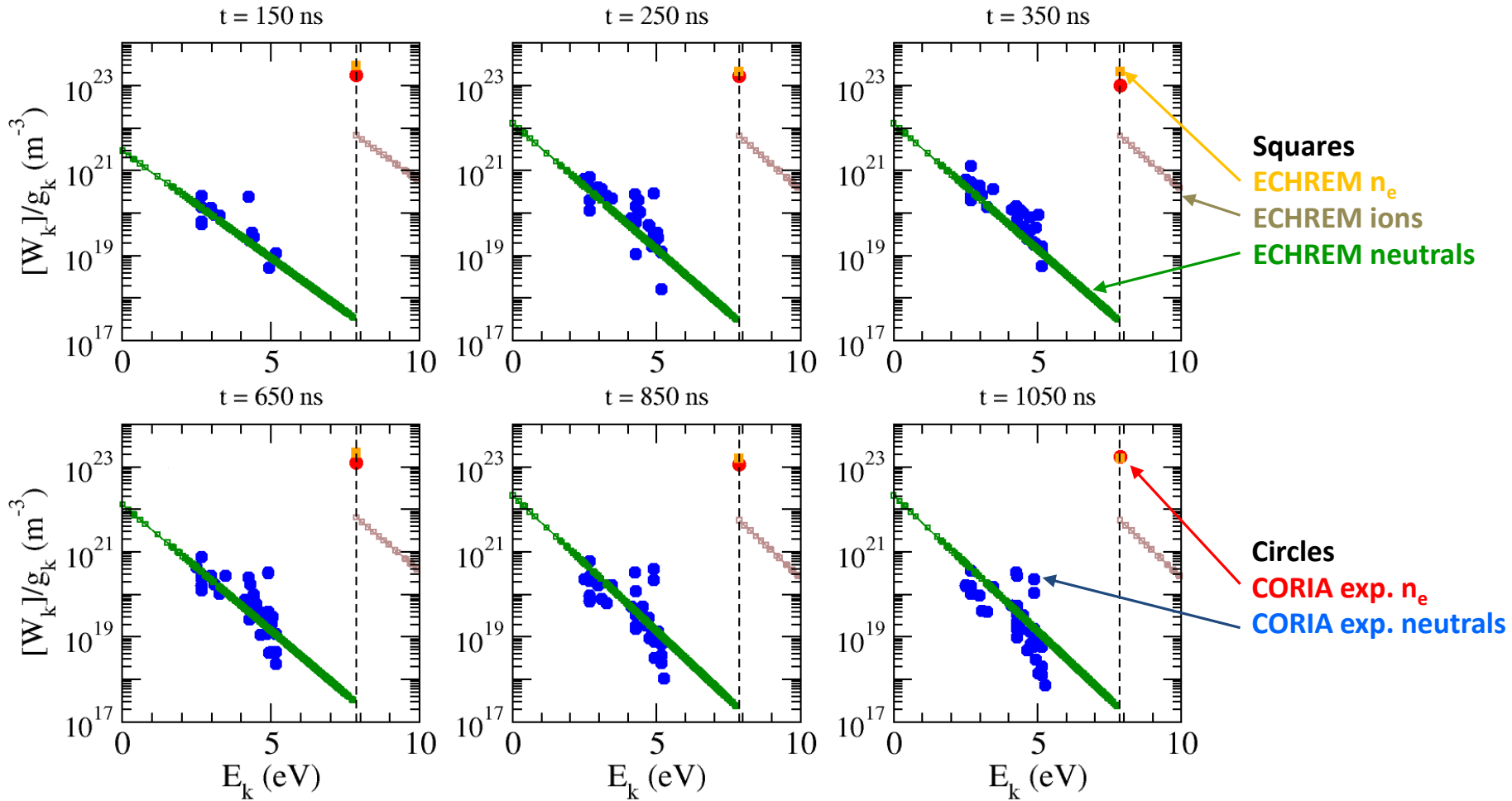
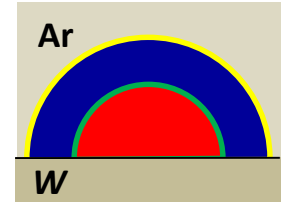
520 000 elementary processes

Radiative Database

NIST, Atomic Line List, ADAS, HULLAC...

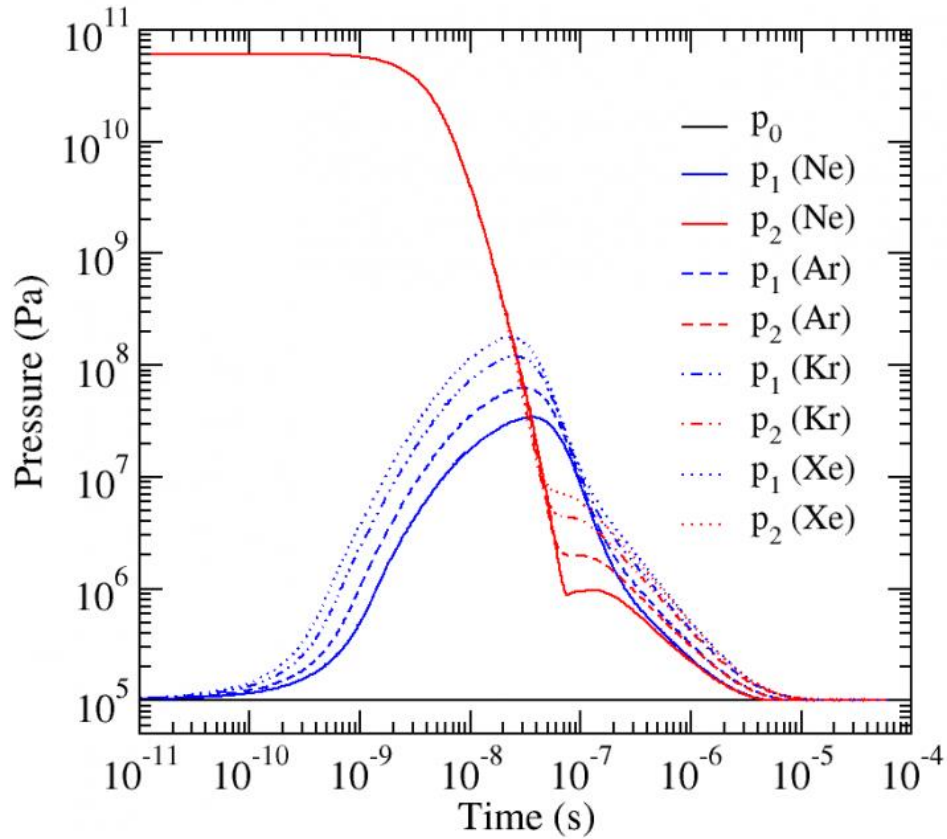
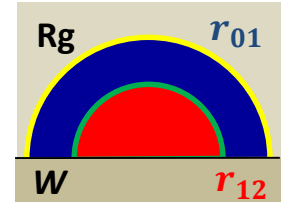
Boltzmann plots

W (Ar, p_{atm}) 30 ps 532 nm 10 J cm⁻²

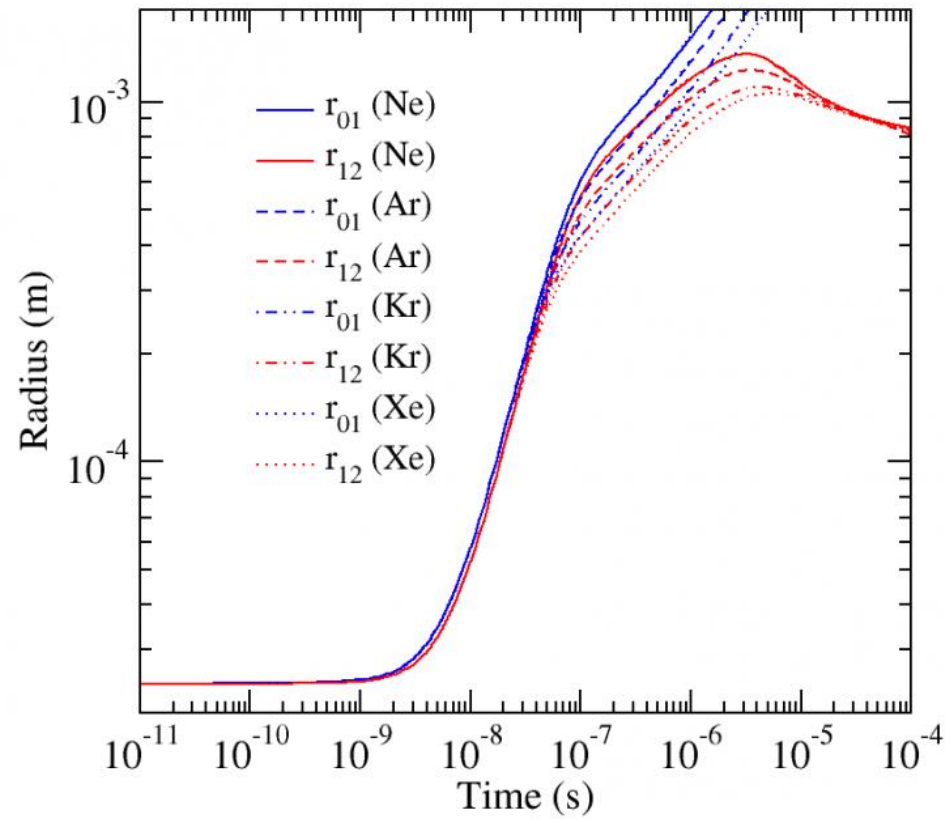


Aerodynamic variables

W (Ar, p_{atm}) 10 ps 532 nm 10 J cm^{-2}



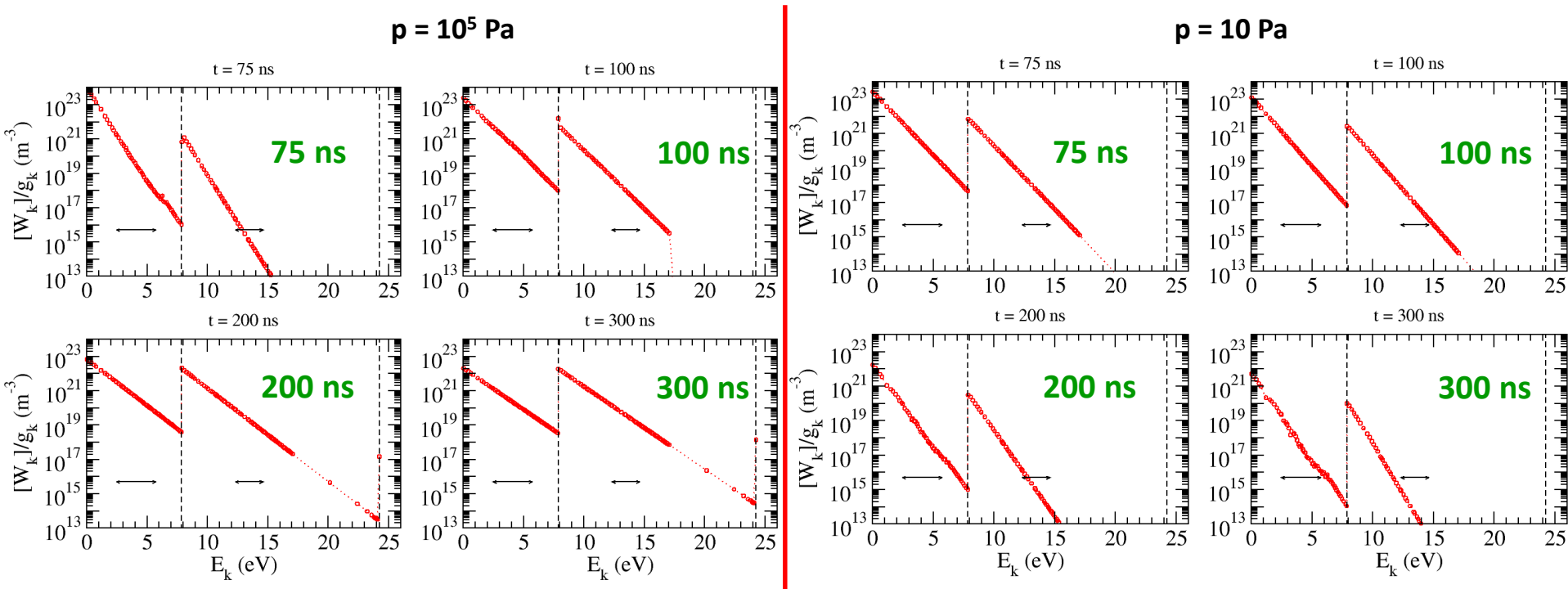
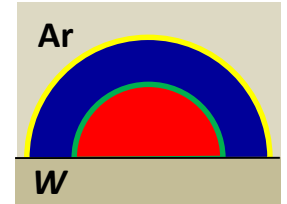
Recompression more efficient with a heavy rare gas
 Ratio of 10 for the pressure at $t \sim 10^{-7}$ s



Radius decreased from 20 % for heavy rare gas
 Better confinement with Xe than with Ne

Boltzmann plots

W (Ar) 10 ps 532 nm 10 J cm⁻²



Excitation non equilibrium

At short times (≈ 75 ns) à 10^5 Pa
 Later (> 200 ns) à 10 Pa

Collision frequency

Spectral lines observation

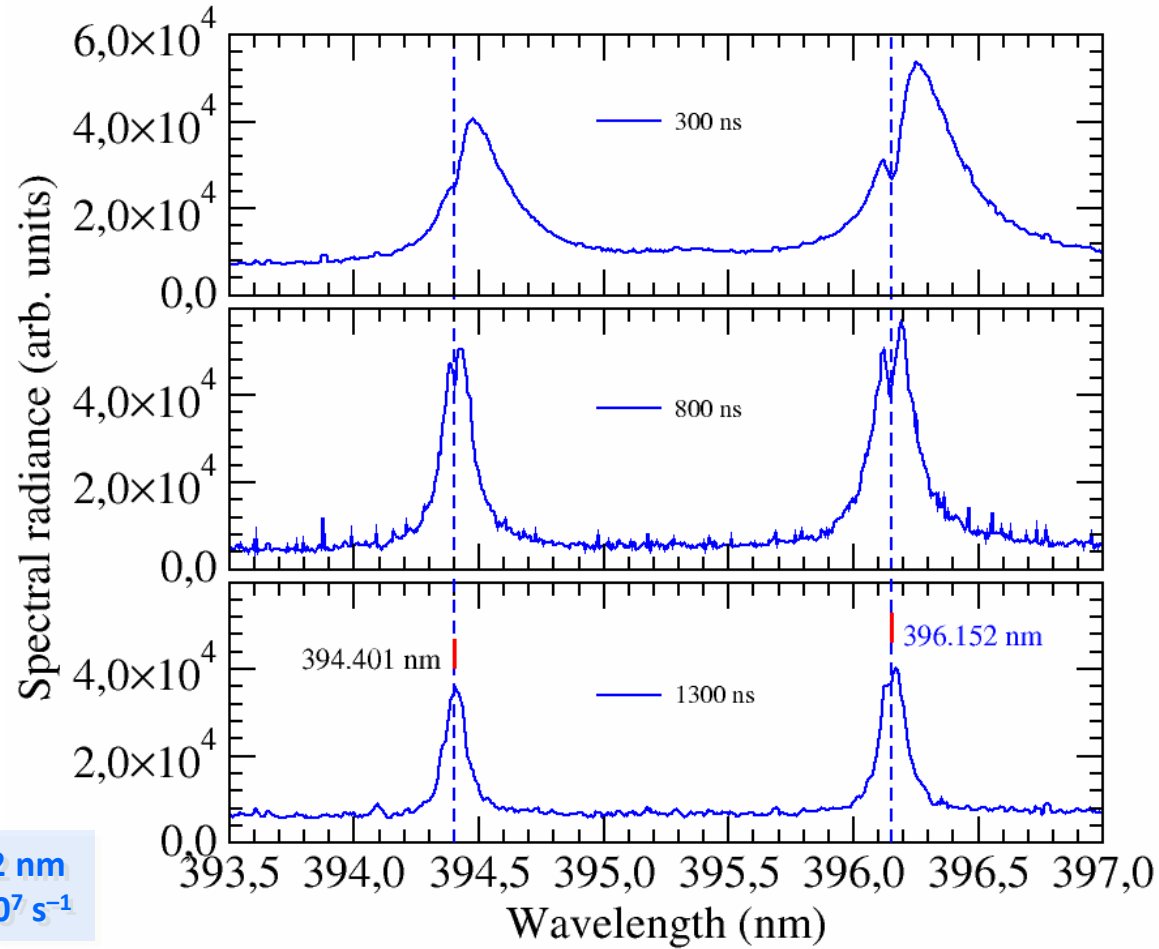
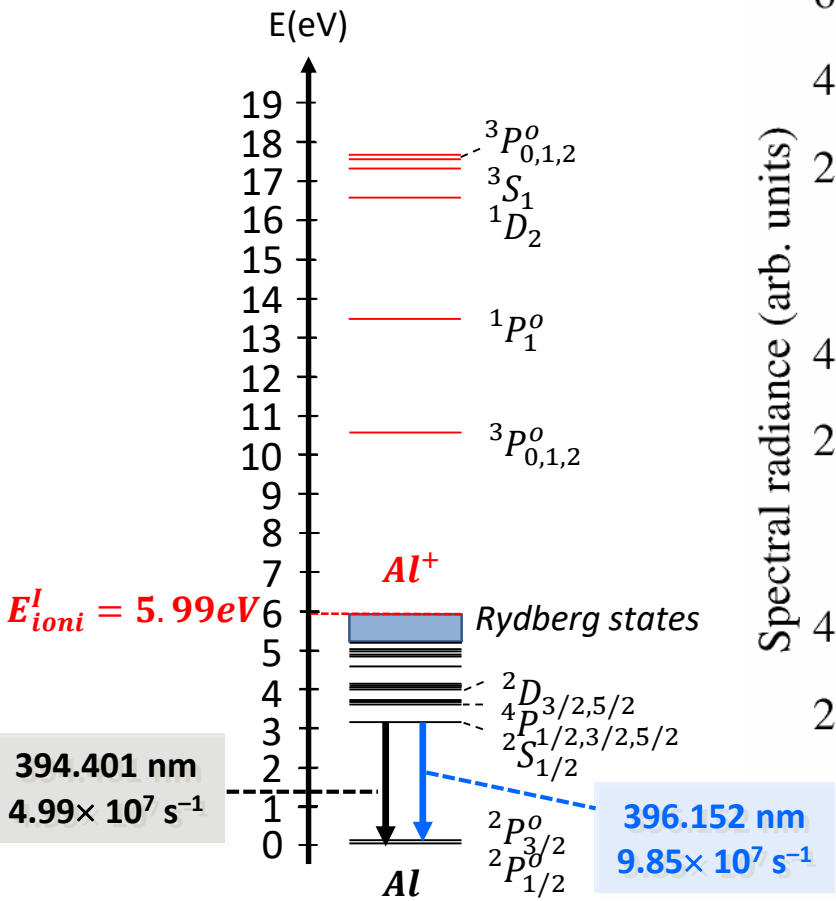
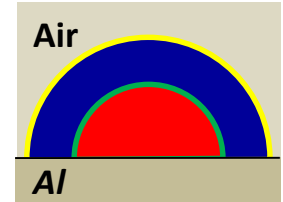
Easy at 10^5 Pa
 Difficult at 10 Pa

Confinement effect

A. Bultel *et al.*
 AIP Conference Proc. **1811** (2017) 120002

Spectra for Al resonance doublet

Al (Air, p_{atm}) 30 ps 1064 nm 10 J cm^{-2}



Stark shift, Stark width and... cold edge re-absorption

Conclusions

1. Entrée Atmosphérique Planétaire

Rôle de la **pression** sur les temps de relaxation

Rôle de la vitesse couplée

2. Plasmas induits par Laser

Influence de la **pression** sur l'ablation

Influence de la **pression** sur le panache

Influence de la **pression** sur le confinement

Influence de la **pression** sur les écarts à l'équilibre

Perspectives

1. Etudes sur l'entrée de la sonde EXOMARS 2020

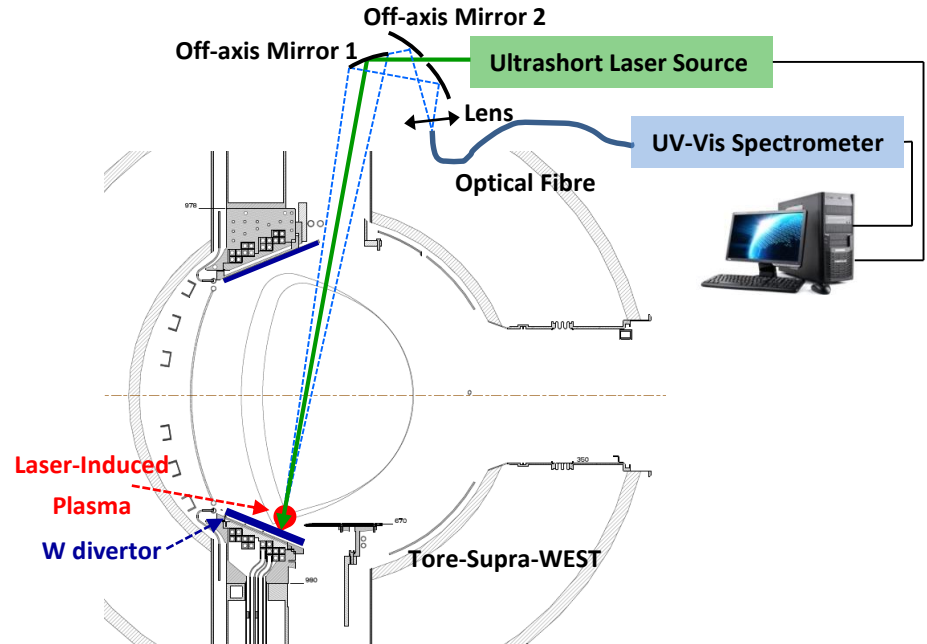
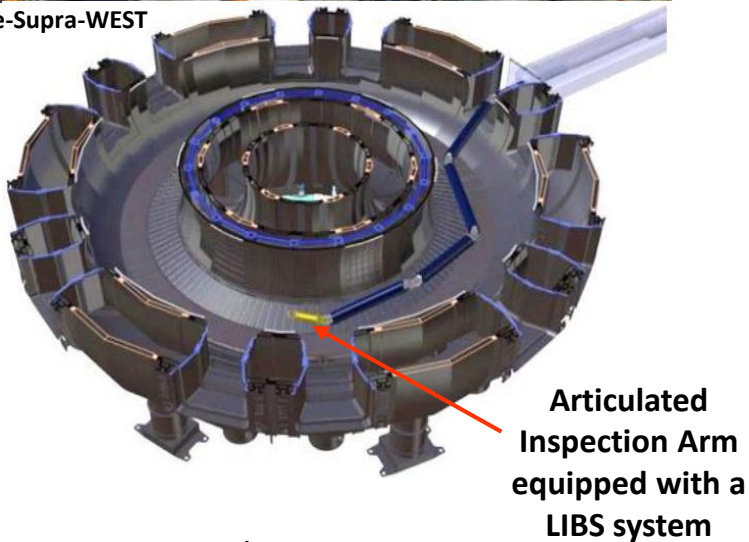
2. Expériences en Double Pulse sur W et Al avec implantation de H and D

3. Tests sur le Tokamak Tore-Supra WEST (CEA Cadarache)

Tore-Supra – WEST



Tore-Supra-WEST



Configuration 1 At the end of the AIA (optical fibres)

Configuration 2 Using off-axis mirrors

Merci de votre attention...

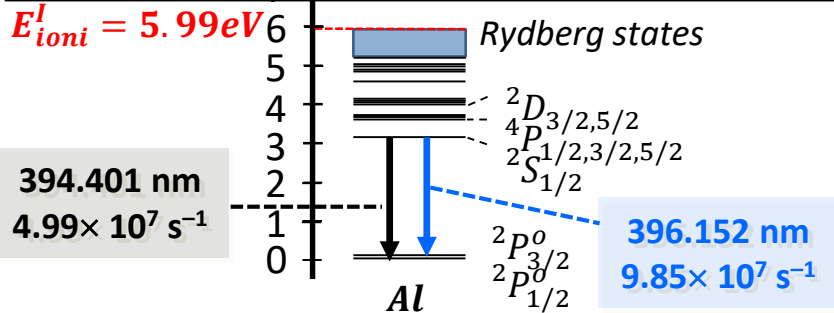
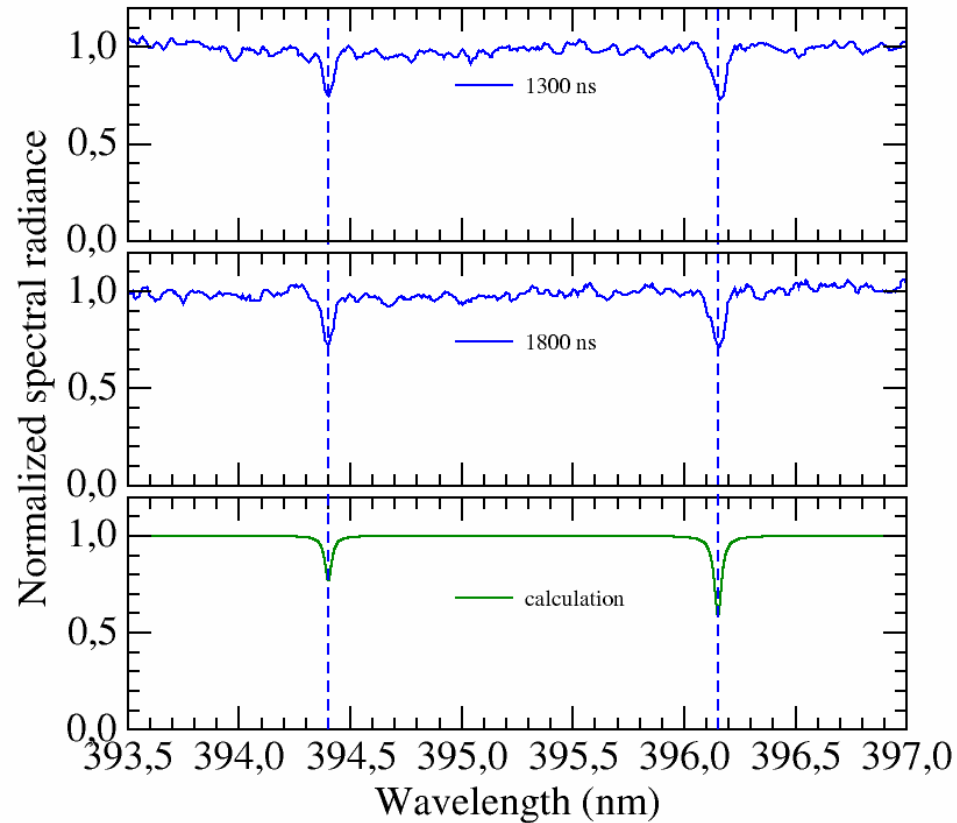
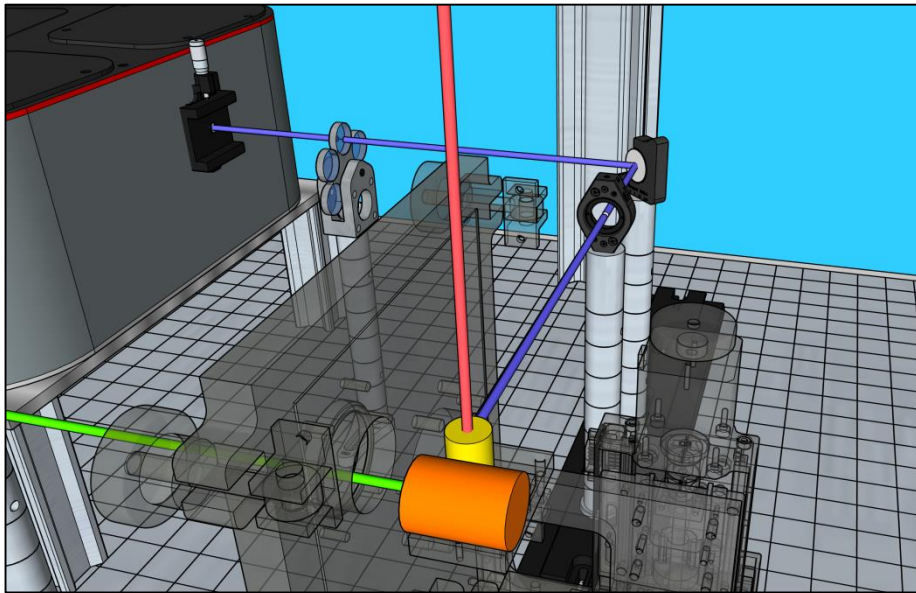
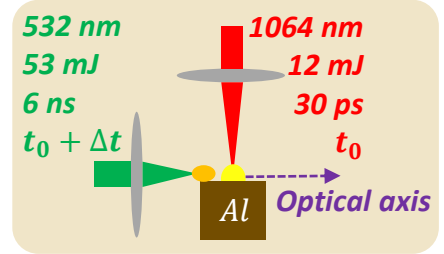


Horizon 2020



Laser-Induced Absorption Spectroscopy LIAS

Al (Air, p_{atm}) 30 ps 1064 nm 10 J cm^{-2}



$$n_e = 2 \times 10^{23} \text{ m}^{-3}$$

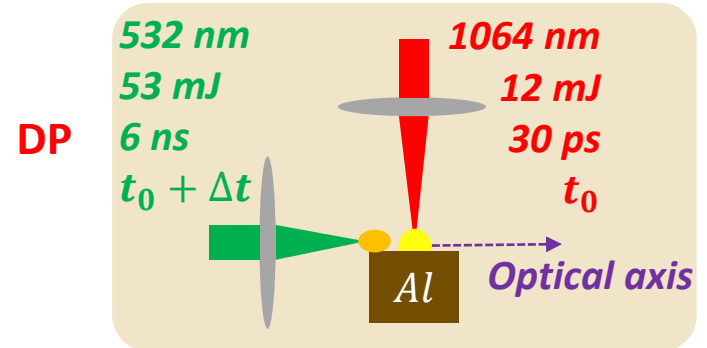
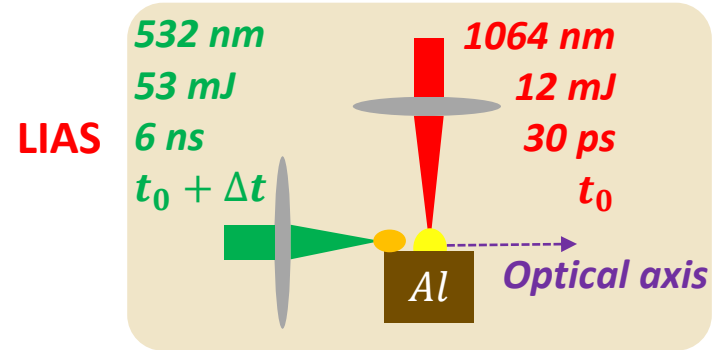
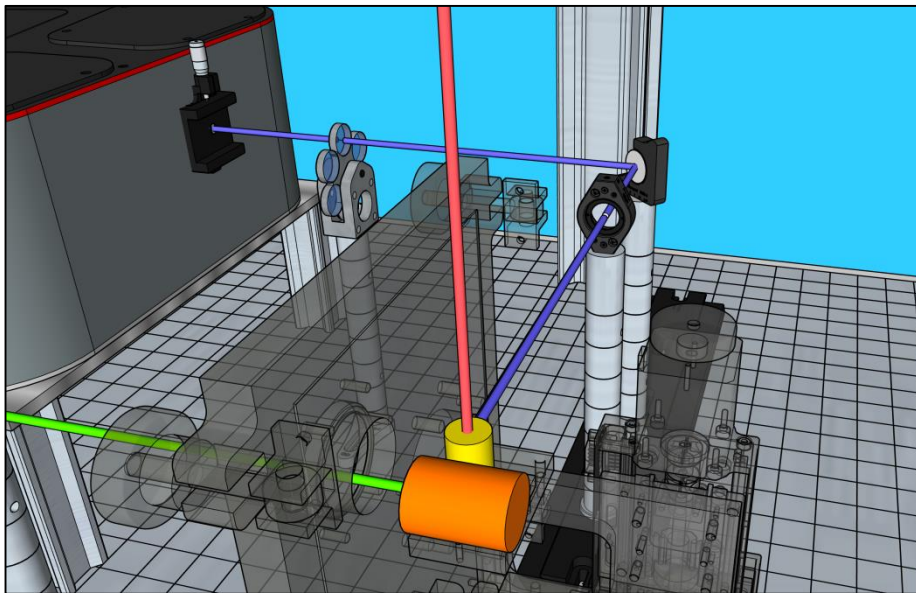
$$T_e = 10\,000 \text{ K}$$

$$[\text{Al}(^2P_{1/2}^0)] = 3.5 \times 10^{20} \text{ m}^{-3}$$

Laser-Induced Absorption Spectroscopy LIAS



DP – Double Pulse Configuration



Inverse Bremsstrahlung !!!

DP – Double Pulse Configuration

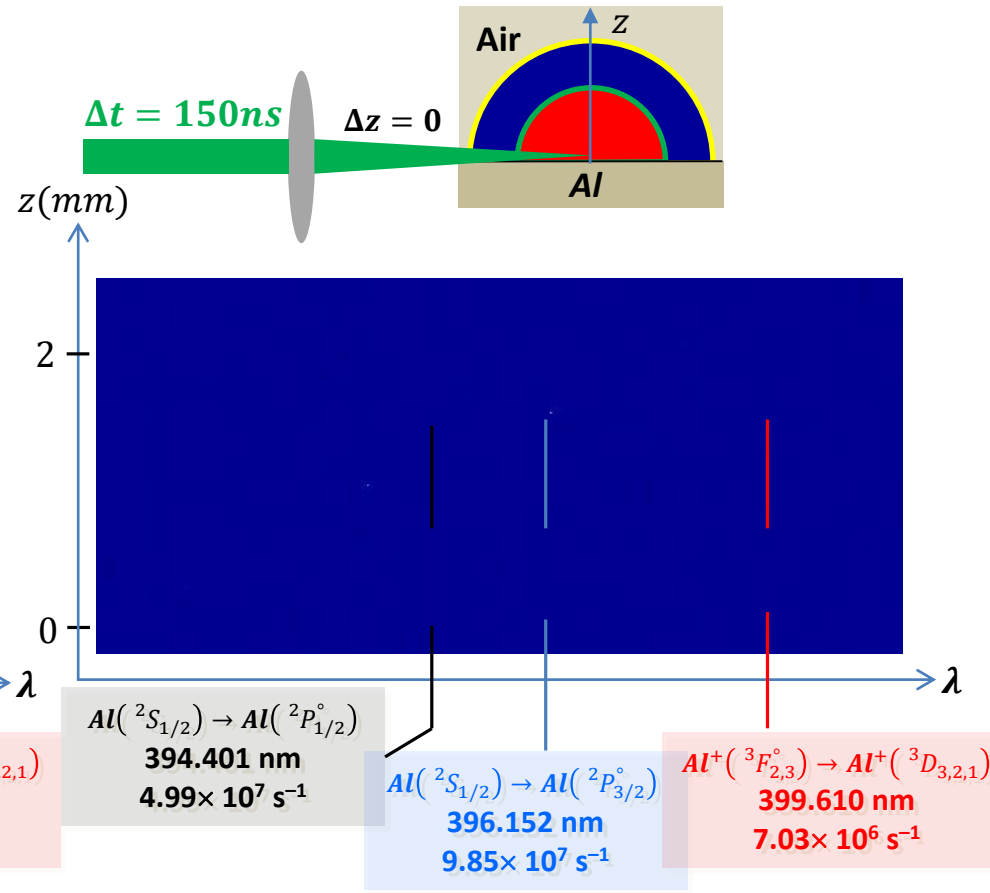
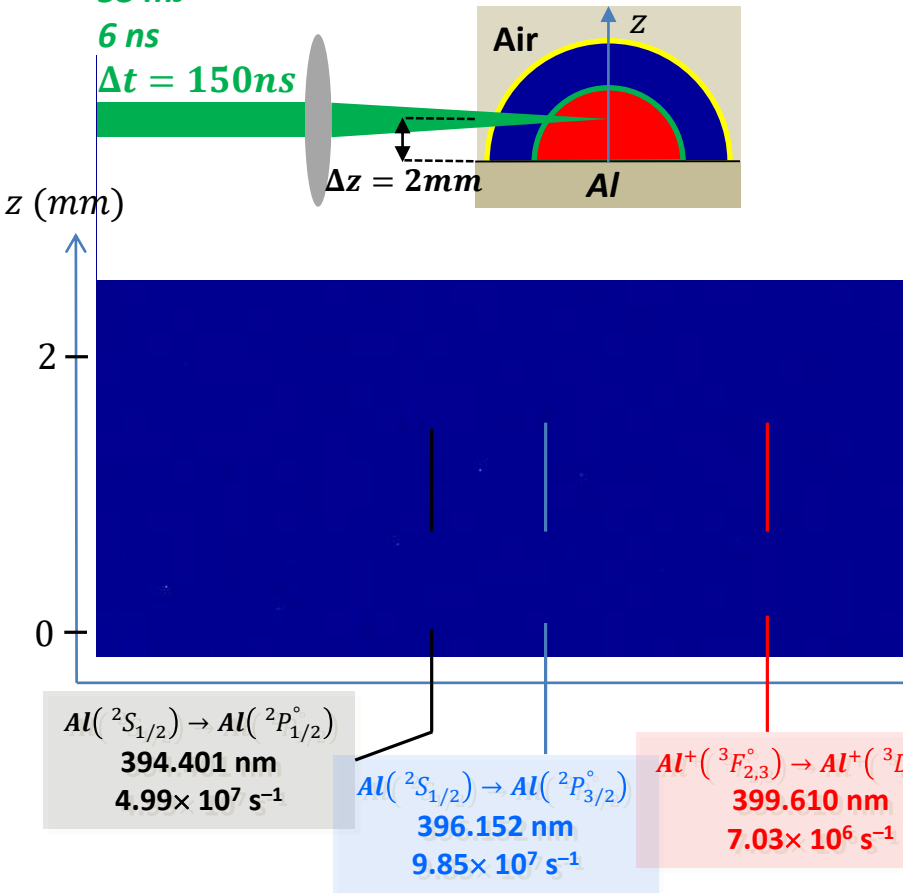
532 nm

53 mJ

6 ns

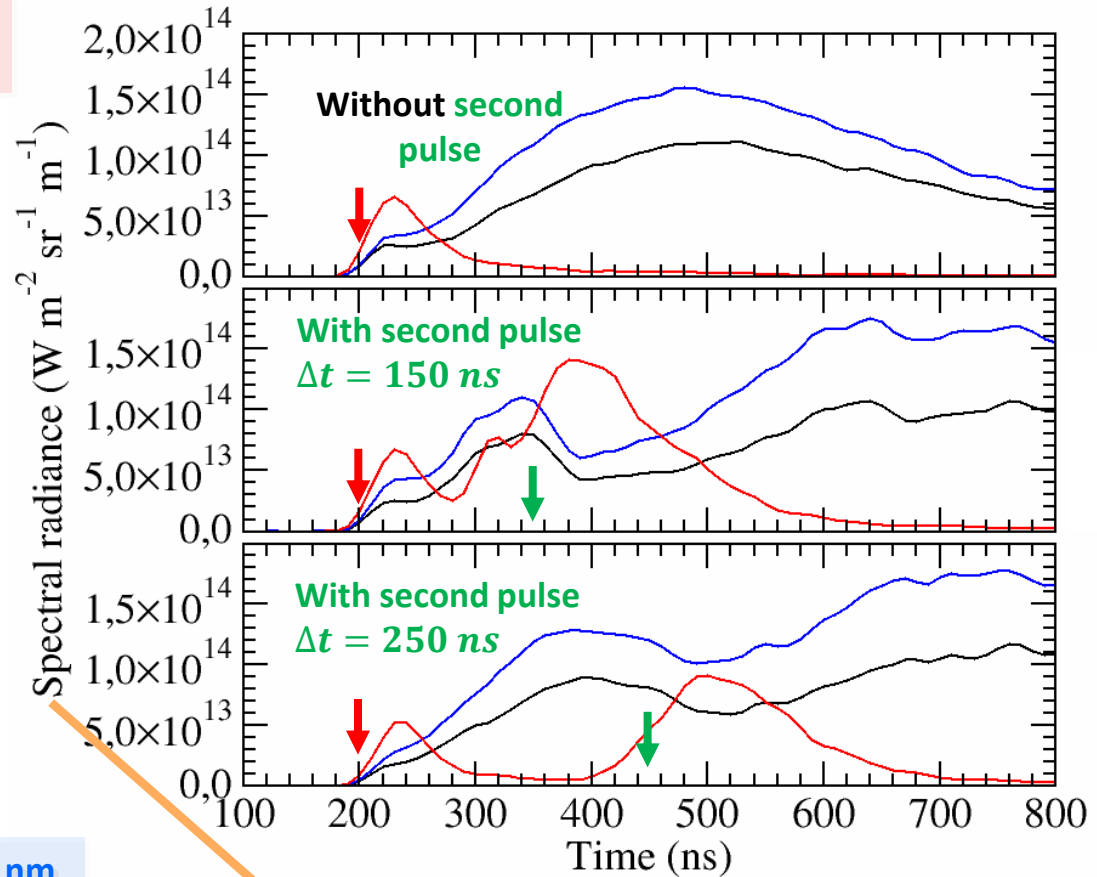
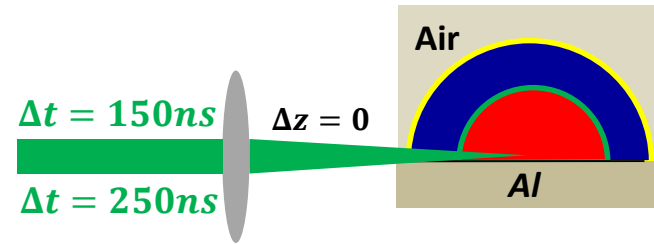
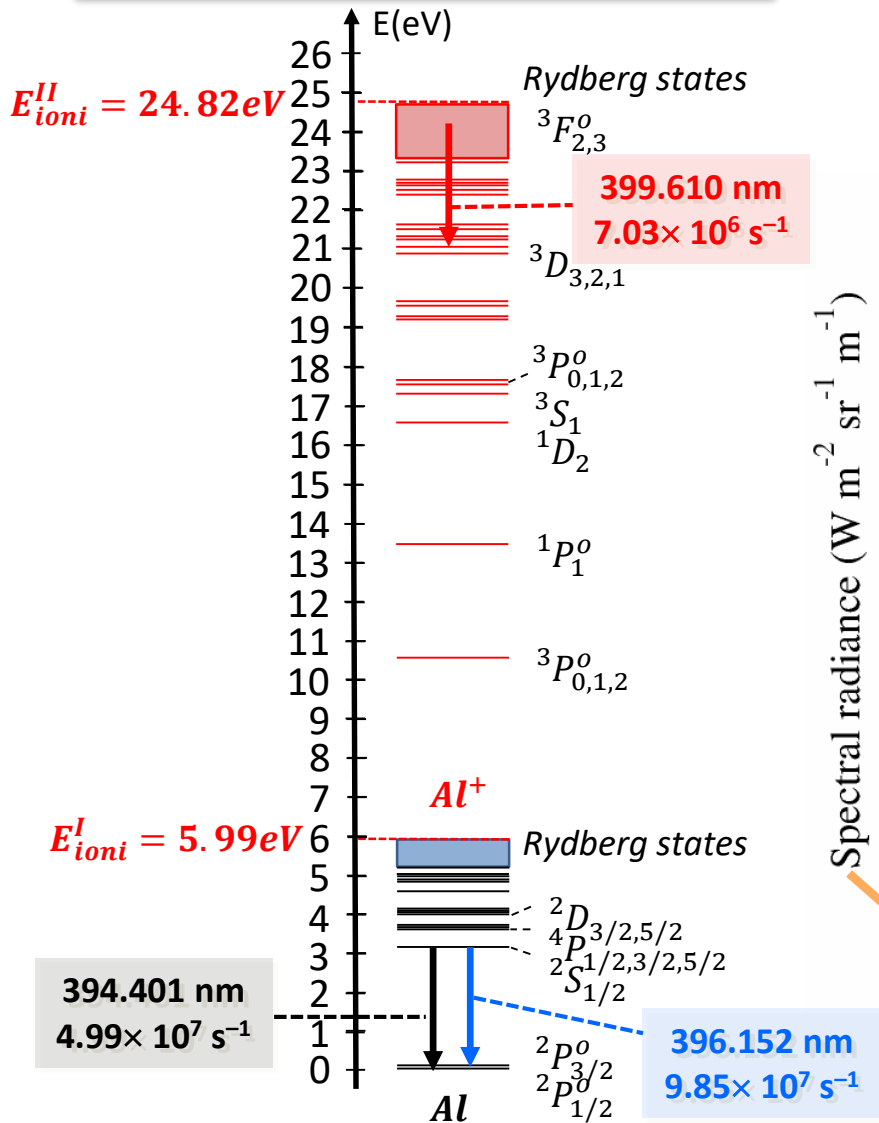
$\Delta t = 150\text{ns}$

Al (Air, p_{atm}) 30 ps 1064 nm 10 J cm^{-2}



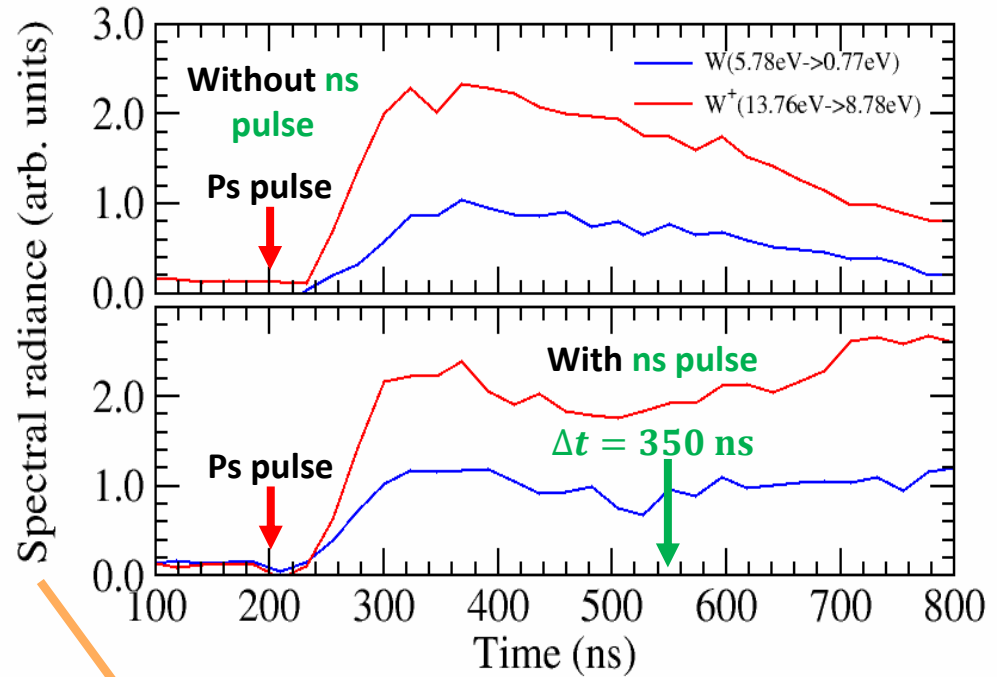
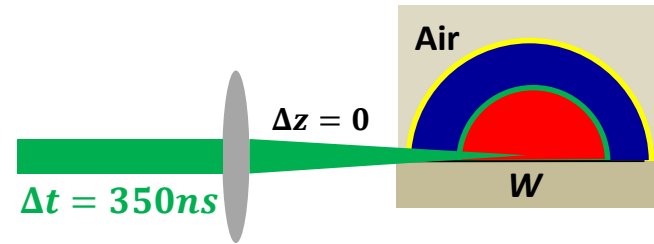
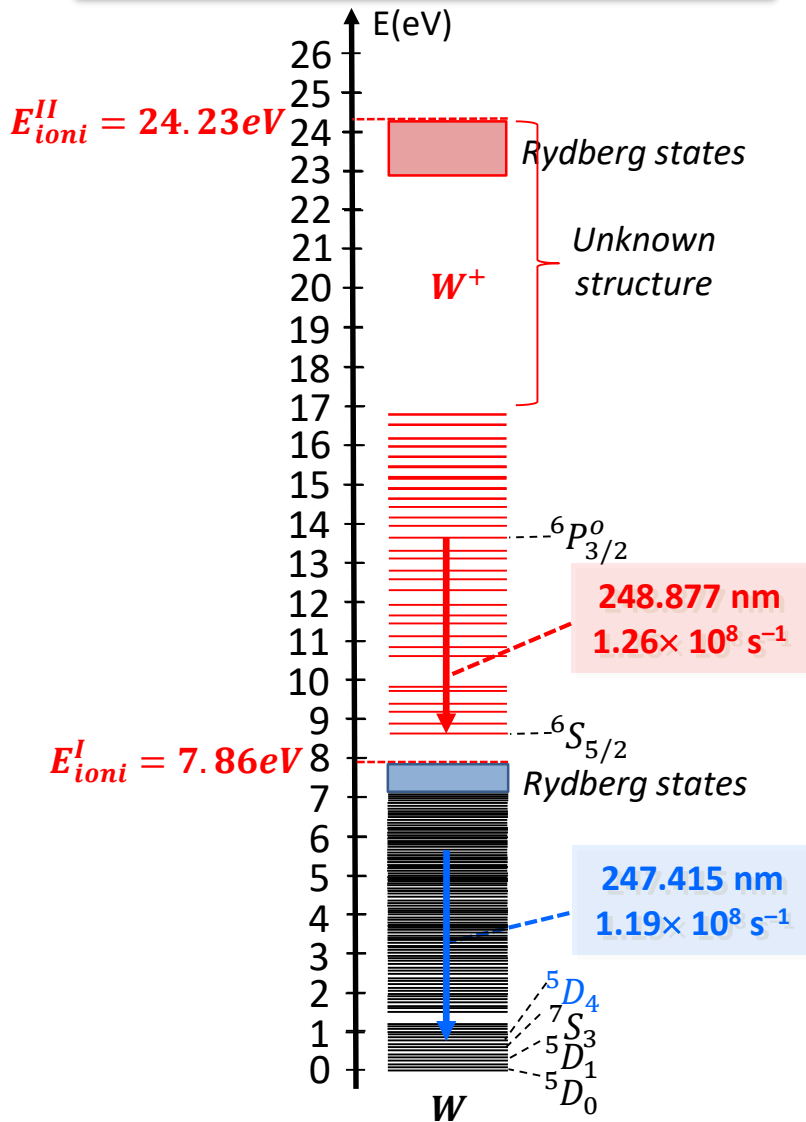
Efficient absorption of the second pulse by the plasma

DP – Double Pulse Configuration



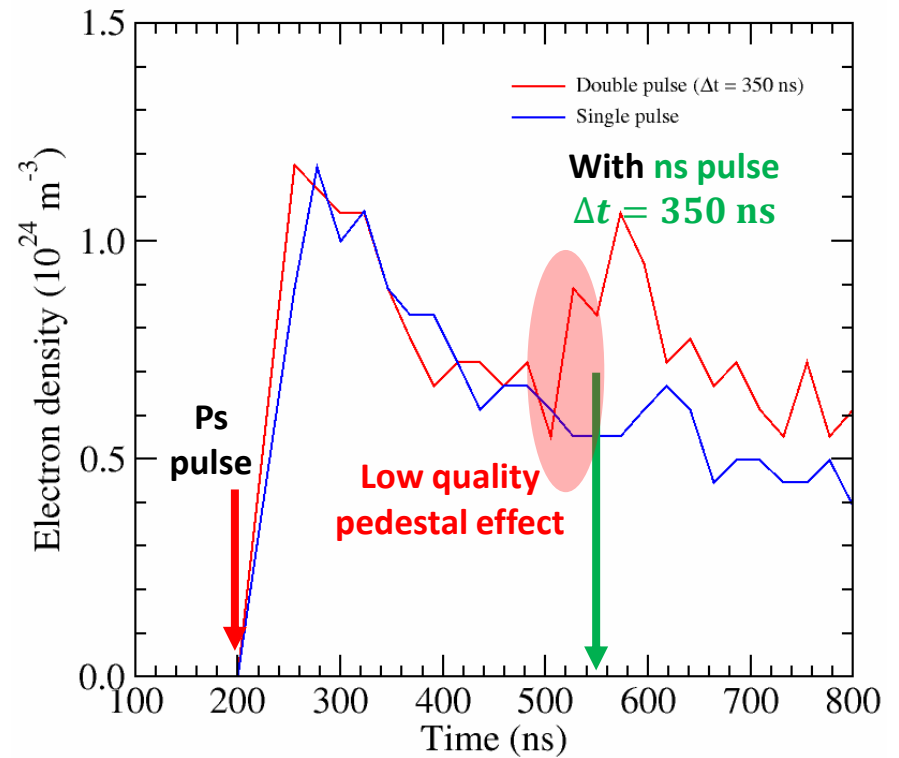
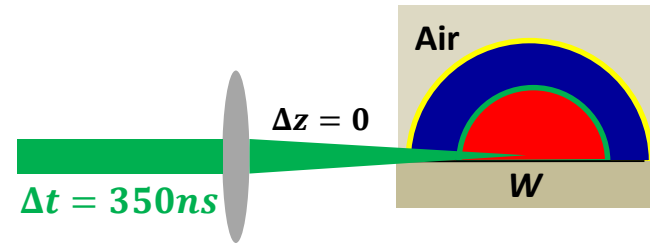
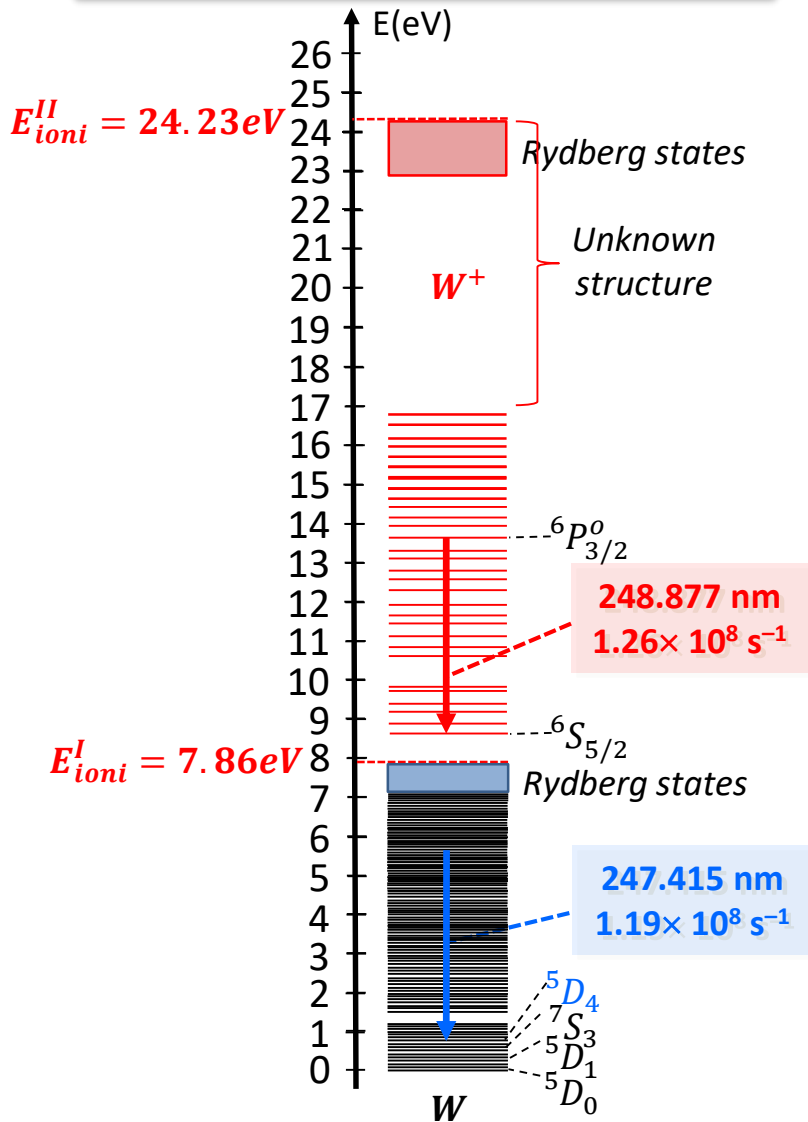
Spectral interval [395, 400] nm

DP – Double Pulse Configuration



Spectral interval [245, 250] nm

DP – Double Pulse Configuration



Consequences on φ_w

Local parietal heat flux φ_w in **chemical non equilibrium**

($\varphi_w \approx 1 - 10 \text{ MW m}^{-2}$)

$$\varphi_w \approx \sum_{\text{Modes } i} k_i \vec{\nabla} T_i \cdot \vec{n}_w + \sum_{\text{Species } j} \gamma_j \beta_j \varphi_j^{(E)} + \int_{\text{Freq. } \nu} \alpha_\nu \iiint_{V_{\text{Plas.}}} \tau_\nu(\vec{r}) \varepsilon_\nu(r) \cos\theta \frac{d^3V}{r^2} d\nu$$

Translation and internal modes Catalysis Radiation

Dependence on the Excited States Number Density

k_i thermal conductivity for mode i

T_i temperature for mode i

γ_j recombination probability for species j

β_j energy accommodation coefficient for species j

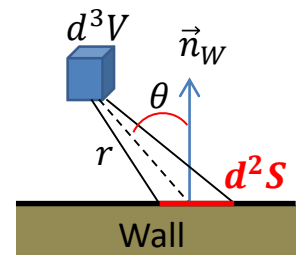
α_ν spectral absorptivity

τ_ν spectral transmittivity along \vec{r}

r distance with d^3V

θ angle with respect to \vec{n}_w

ε_ν spectral emission coefficient



Thermochemical non equilibrium

Excited states population density

(Species X on an excited state m)

$$\frac{\partial [X_m]}{\partial t} + \vec{\nabla} \cdot ([X_m] \vec{u} + \vec{J}_{X_m}) = \left(\frac{\partial [X_m]}{\partial t} \right)_{Coll.} + \left(\frac{\partial [X_m]}{\partial t} \right)_{Rad.}$$

Convection..... τ_{Conv}

Diffusion..... τ_{Diff}

Collisional-radiative..... τ_{CR}

Damkhöler numbers

$$\left(\frac{\partial [X_m]}{\partial t} \right)_{Coll.} \gg \left(\frac{\partial [X_m]}{\partial t} \right)_{Rad.}$$

$$Da_1 = \frac{\tau_{Conv}}{\tau_{CR}}$$

$$Da_2 = \frac{\tau_{Conv}}{\tau_{MB}}$$

$$Da_3 = \frac{\tau_{Conv}}{\tau_{e-h}}$$

Chemical equilibrium $Da_1 \gg 1$

Chemical non equilibrium $Da_1 \approx 1$

Frozen flow $Da_1 \ll 1$

$Da_2 \gg 1$

Translation equilibrium **Thermal non equilibrium**

$Da_3 \leq 1$

Excitation non equilibrium

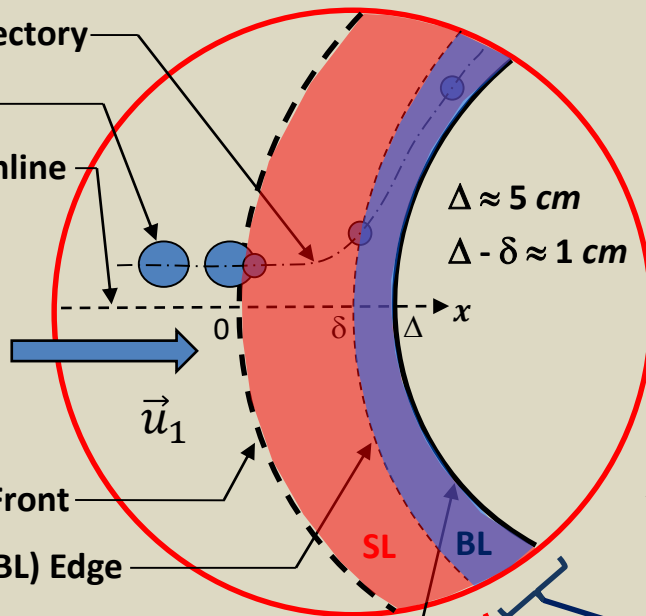
Planetary Atmospheric Entry

(u_1 5 to 15 $km\ s^{-1}$)

Fluid particle trajectory

Fluid particle

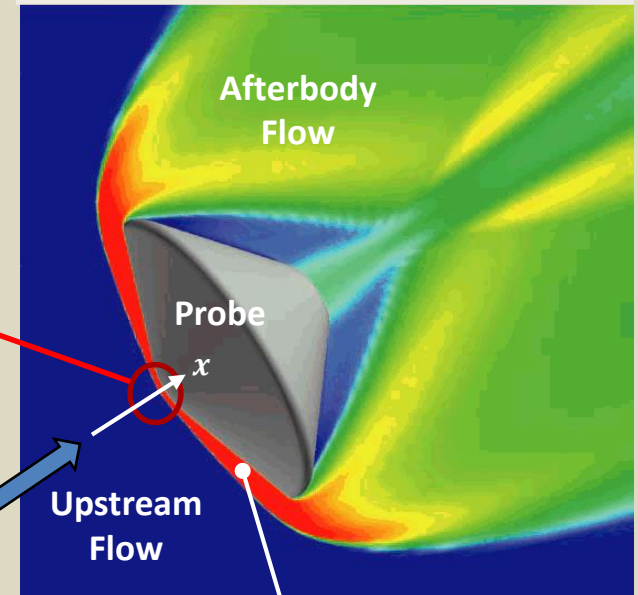
Stagnation streamline



Detached Shock Front

Boundary Layer (BL) Edge

Thermal Protection System (TPS)



Upstream Flow

Shock Layer (SL)

SL Dissociation and Ionisation

Under-population for involved excited states

BL Recombination

Over-population for involved excited states

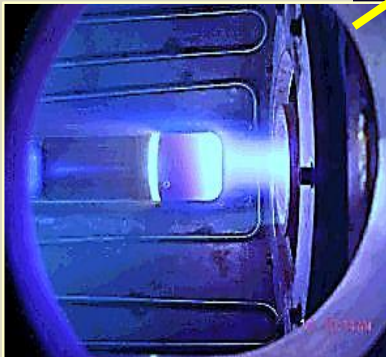
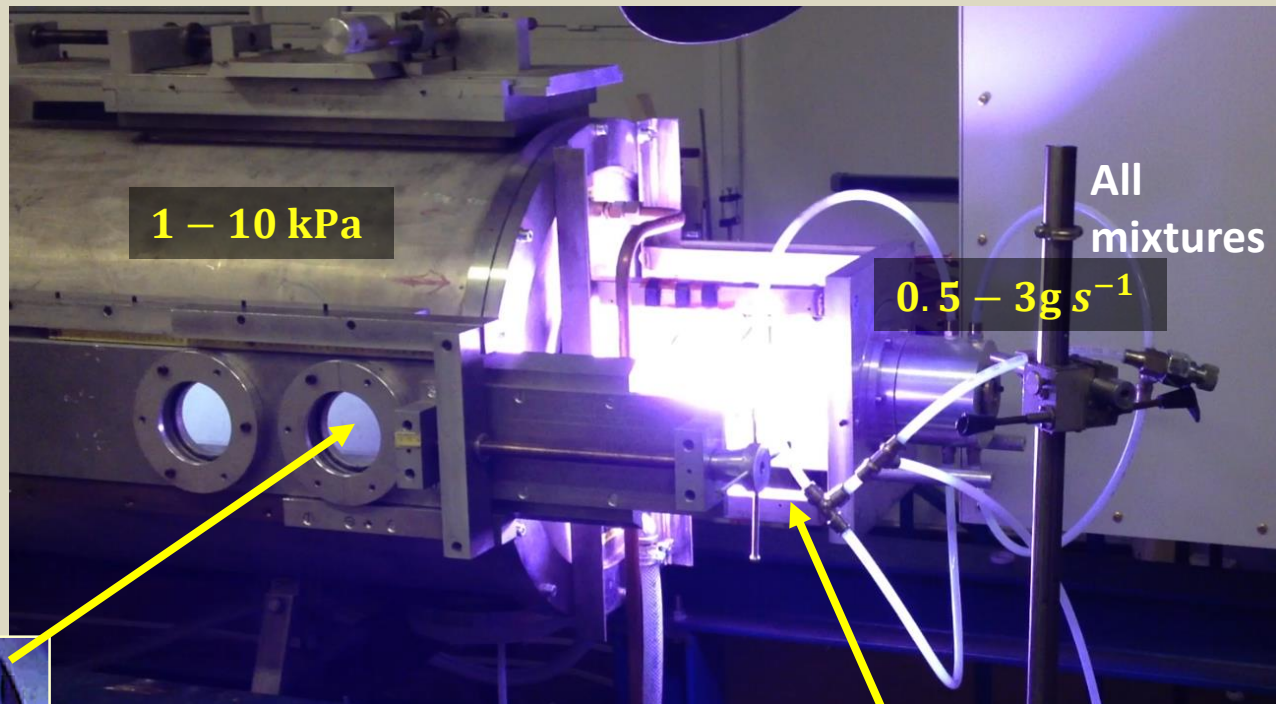
Departure from excitation equilibrium

and possible influence of radiation

Validation of CoRaM-MARS and RH1D codes?

High Enthalpy Wind Tunnel

SOUPLIN – CORIA



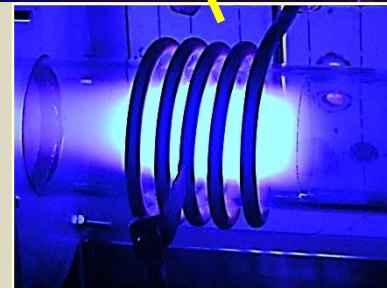
Parietal temperature and heat flux

Thermal sensor, IR Thermography

Emission, absorption spectroscopy

Laser (Absorption, LiF) BL probing

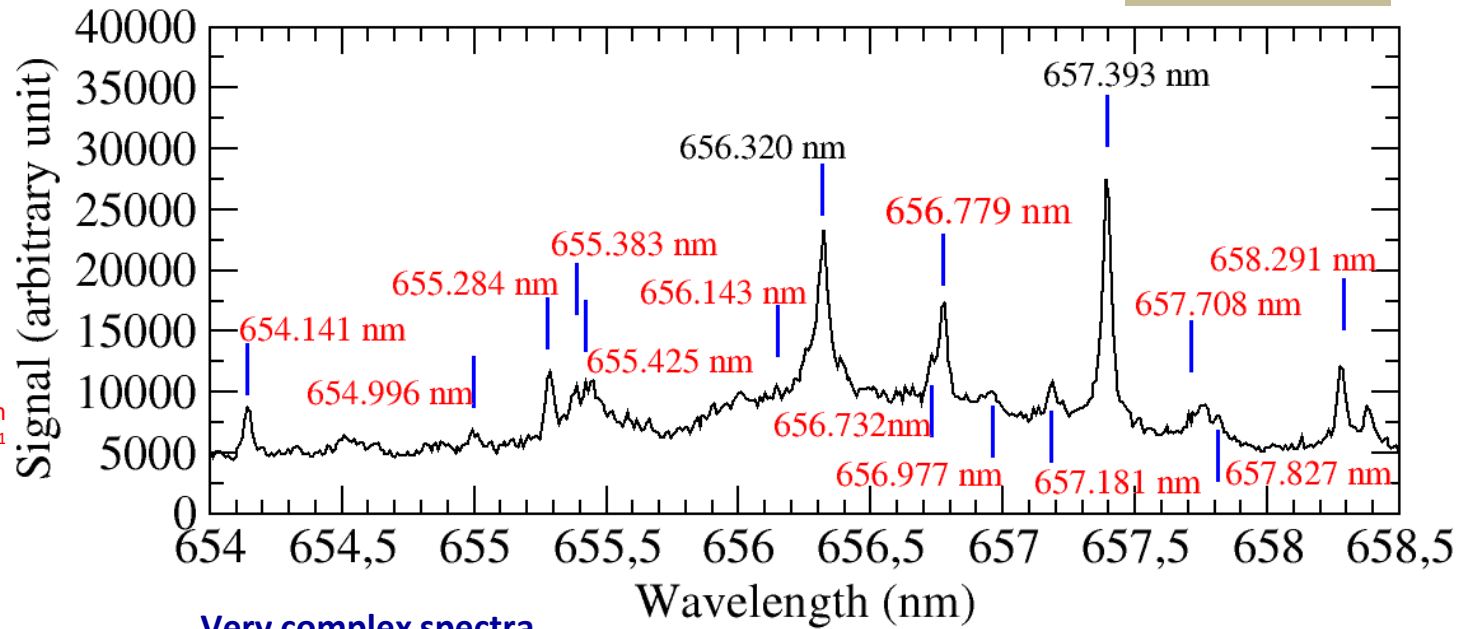
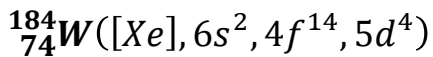
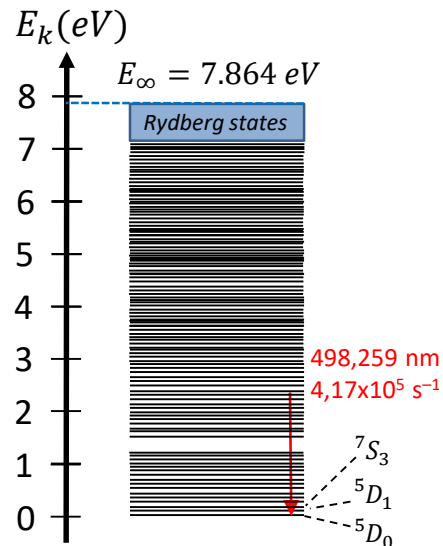
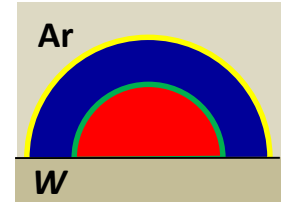
***LIBS probing of the sample** (C – SiC...)*



1.76 MHz

60 kW

Spectroscopic analysis



Very complex spectra...

Lines broadened by Stark effect

Few lines with known A_{ki} ...

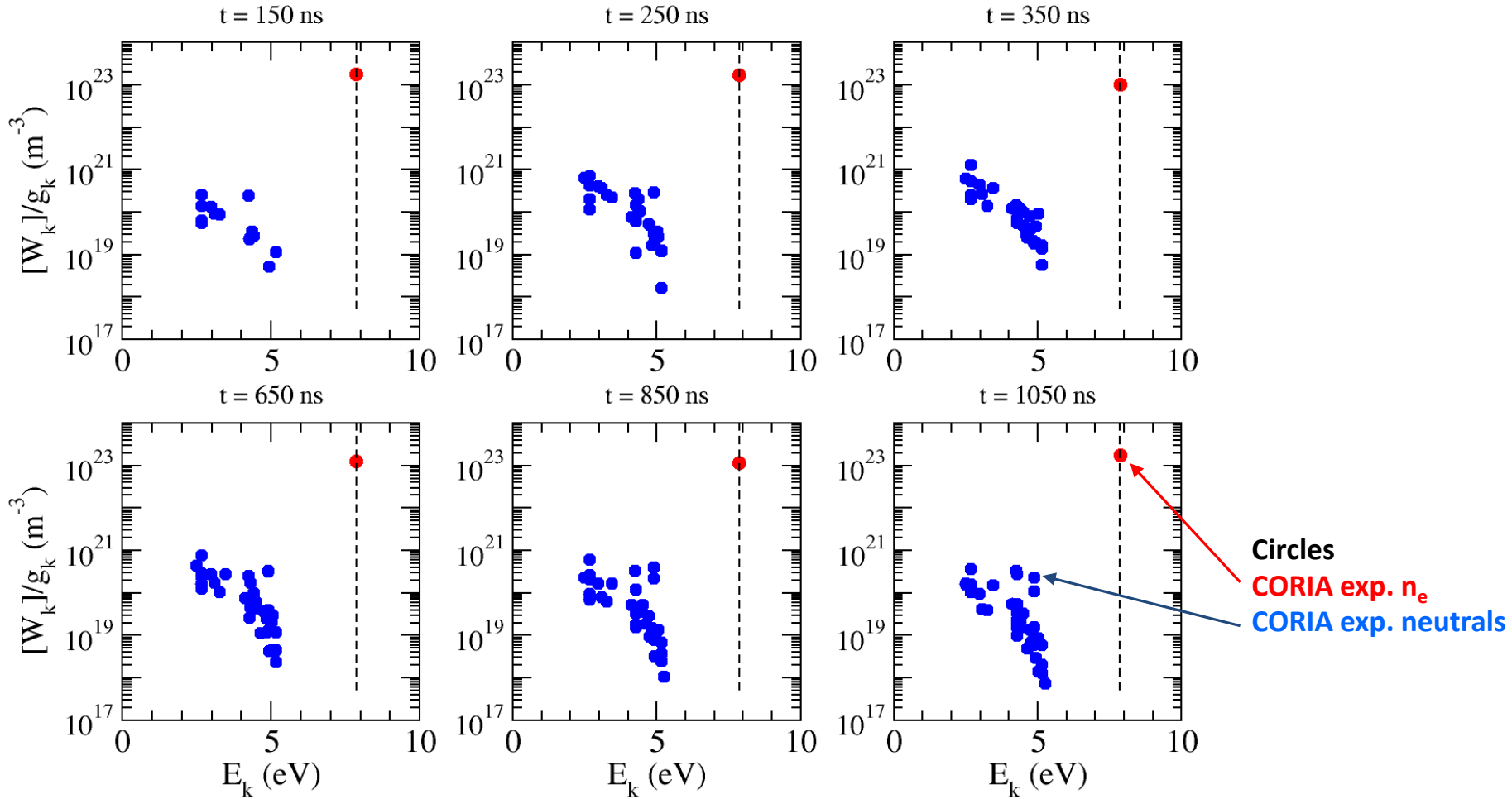
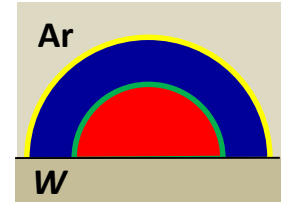
W I transitions reported in the NIST database with A_{ki} 7 %

W II transitions reported in the NIST database with A_{ki} 7 %

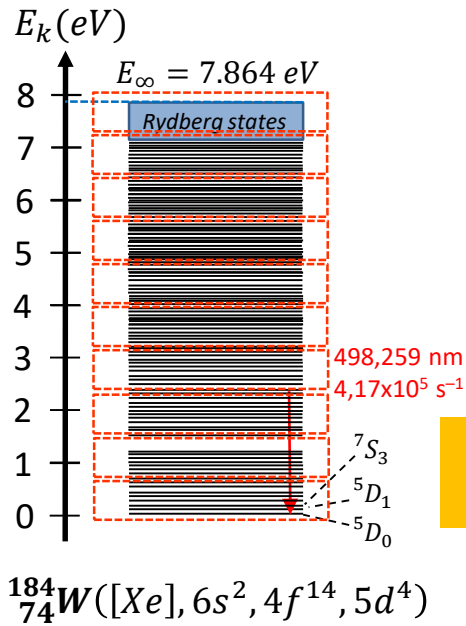
W III transitions reported in the NIST database with A_{ki} 1 %

Boltzmann plots

W (Ar, p_{atm}) 30 ps 532 nm 10 J cm⁻²



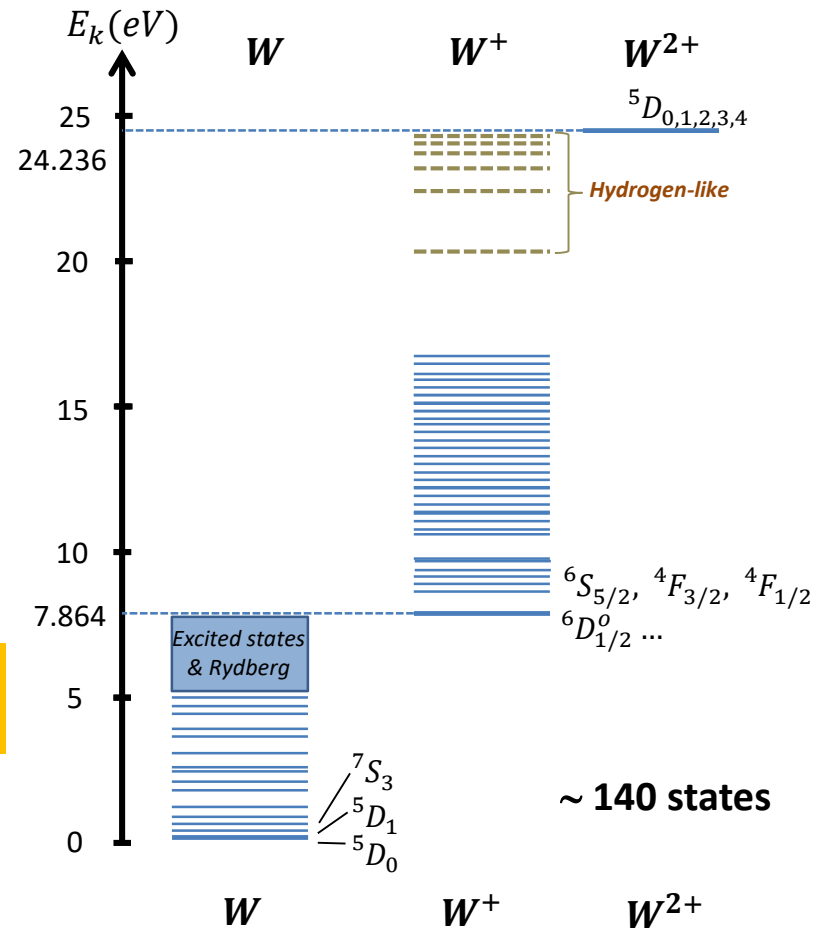
Simplification of the energy diagram



Number of states reported in the NIST database:

- 508 for W
- 264 for W^+

Lumping of levels
 $\Delta E \sim 0.1 eV$

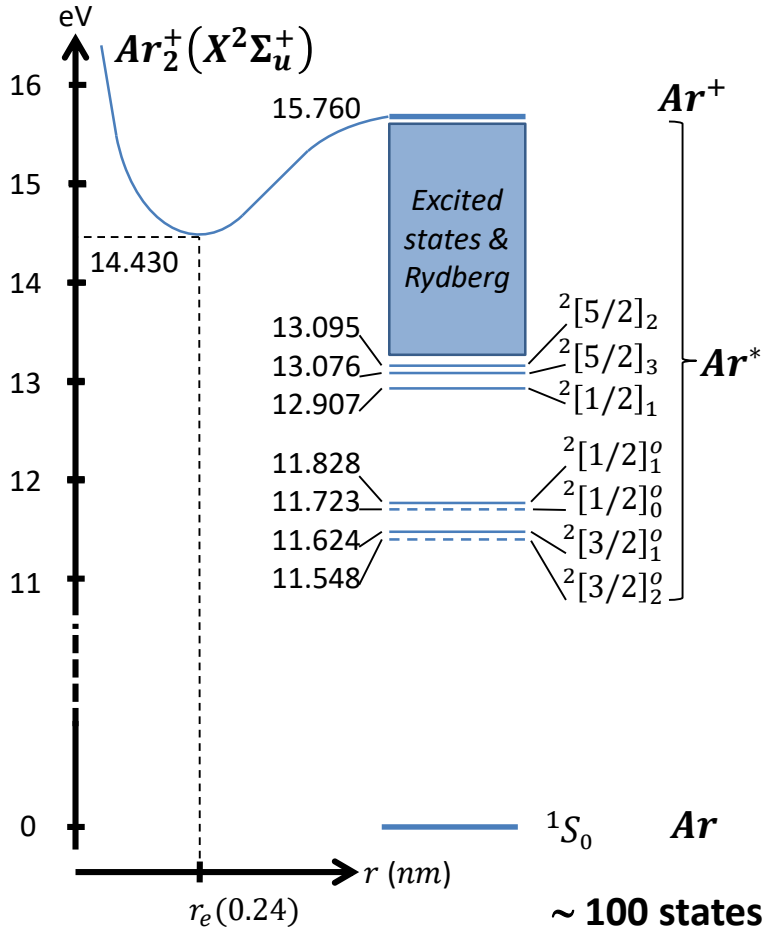


Type 3 spe. ~ 140 states

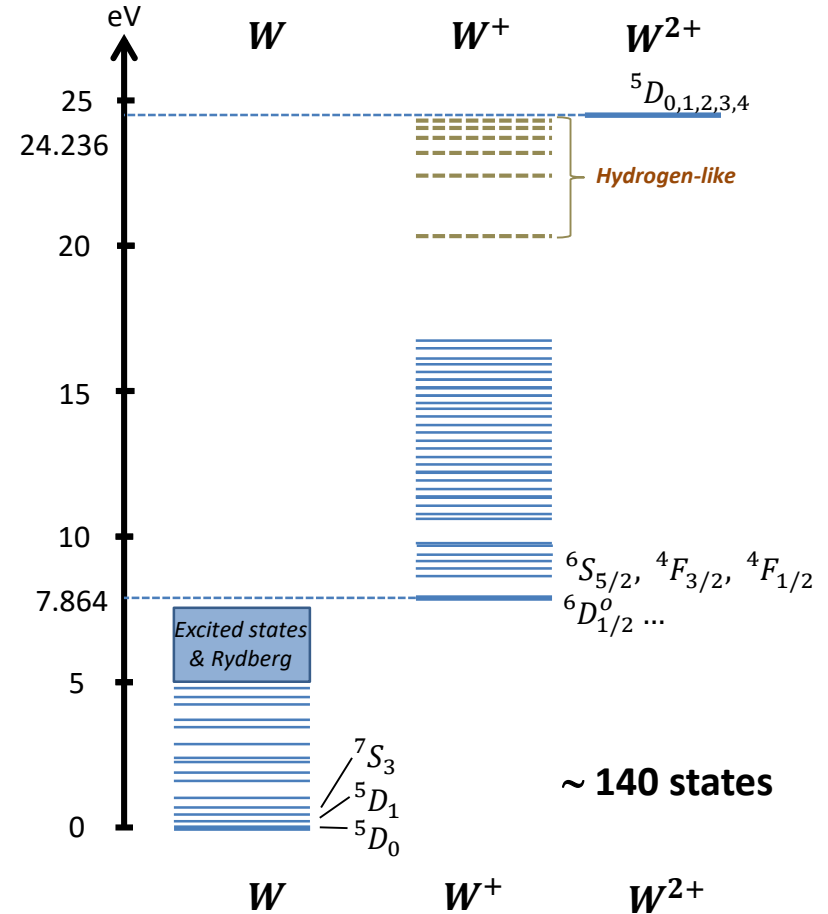
Type	3 spe.	~ 140 states
Atoms	W	$5D_0, 5D_1, 5D_2, 5D_3 \dots$ (60 states)
Ions	W^+	$6D_{1/2}, 6D_{3/2}, 6D_{5/2}, 6D_{7/2}, \dots$ (74 states)
	W^{2+}	$5D_{0..4}, 3P_{2_{0..2}}, 5F_{1..5}, 6D_{7/2}, \dots$ (5 states)

Example $W - Ar$

Shock layer - Argon



Central plasma - Tungsten



Type 3 spe. ~ 100 states

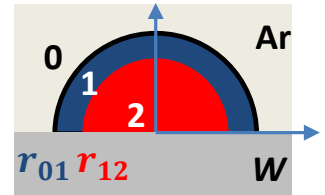
Mol. ions	Ar_2^+	$X^2\Sigma_u^+$	
Atoms	Ar	$1S_0$, $2[3/2]_2^o$, $2[3/2]_1^o$, $2[1/2]_0^o$,	(90 states)
Atomic ions	Ar^+	$2P_{3/2}^o$, $2P_{1/2}^o$, $2S_{1/2}$, $4D_{7/2}$,	(7 states)

Type 3 spe. ~ 140 states

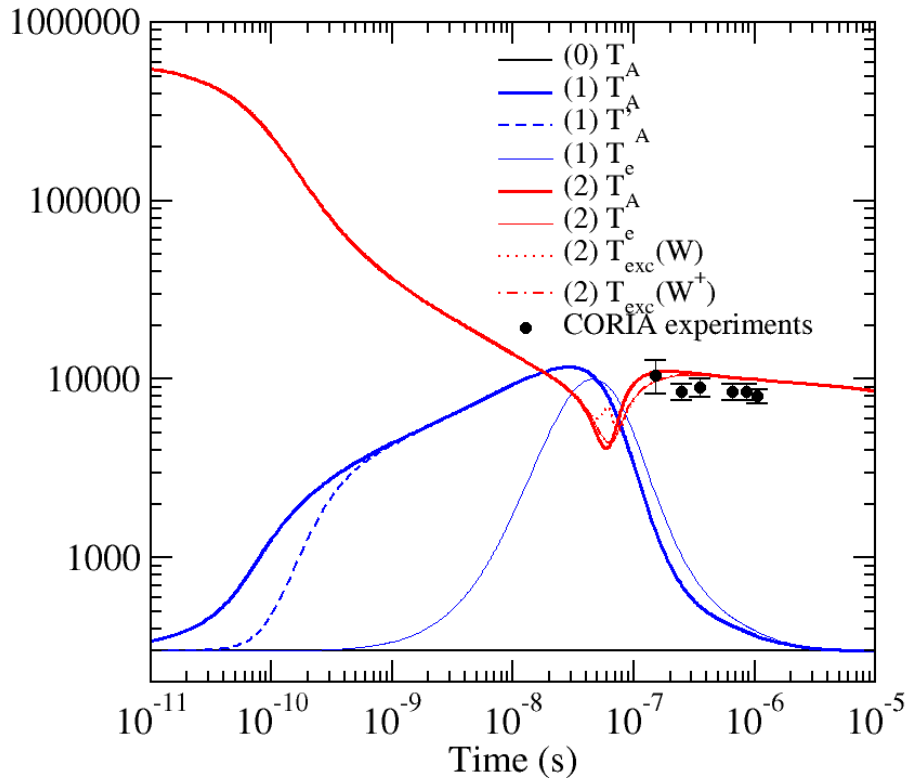
Atoms	W	$5D_0$, $5D_1$, $5D_2$, $5D_3$	(60 states)
Ions	W^+	$6D_{1/2}$, $6D_{3/2}$, $6D_{5/2}$, $6D_{7/2}$,	(74 states)
	W^{2+}	$5D_{0...4}$, $3P_{2...2}$, $5F_{1...5}$, $6D_{7/2}$,	(5 states)

Influence of the background gas pressure

W (Ar) 10 ps 532 nm 10 J cm⁻²

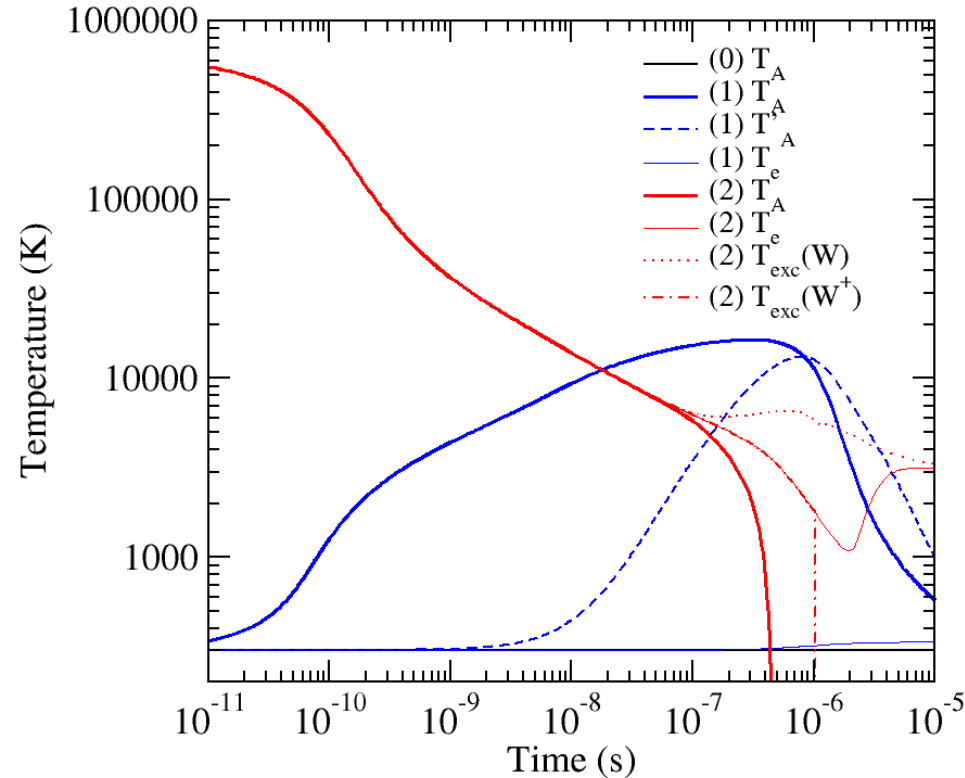


p = 10⁵ Pa



Long lifetime of the plasma

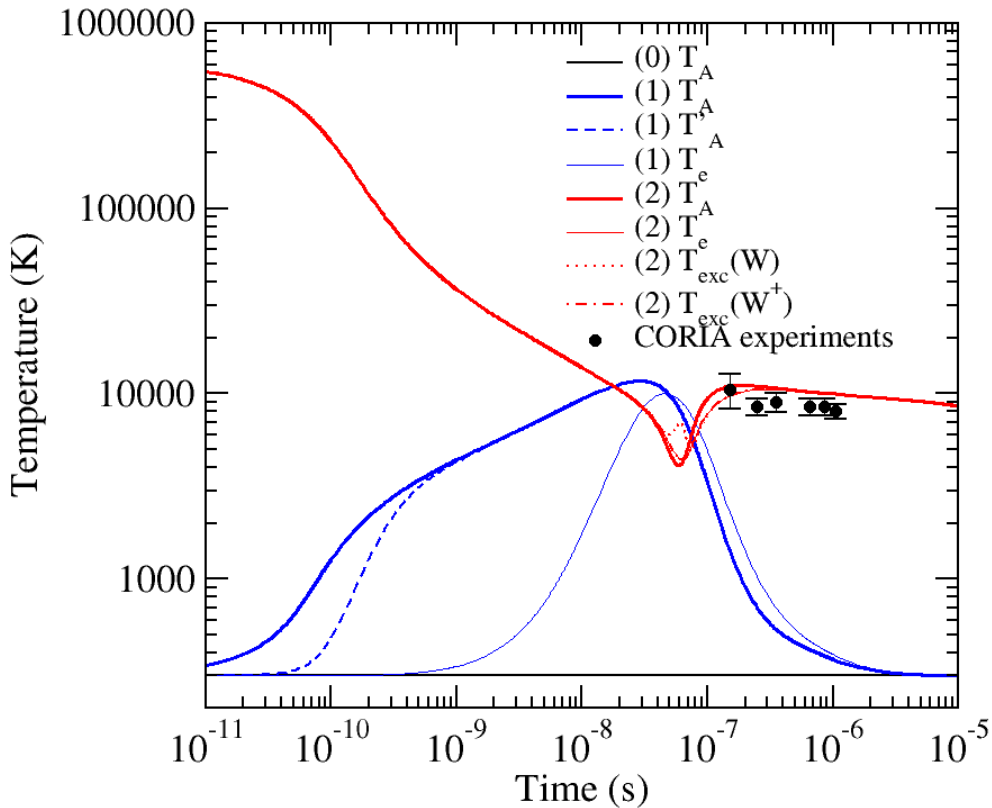
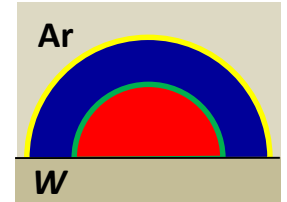
p = 10 Pa



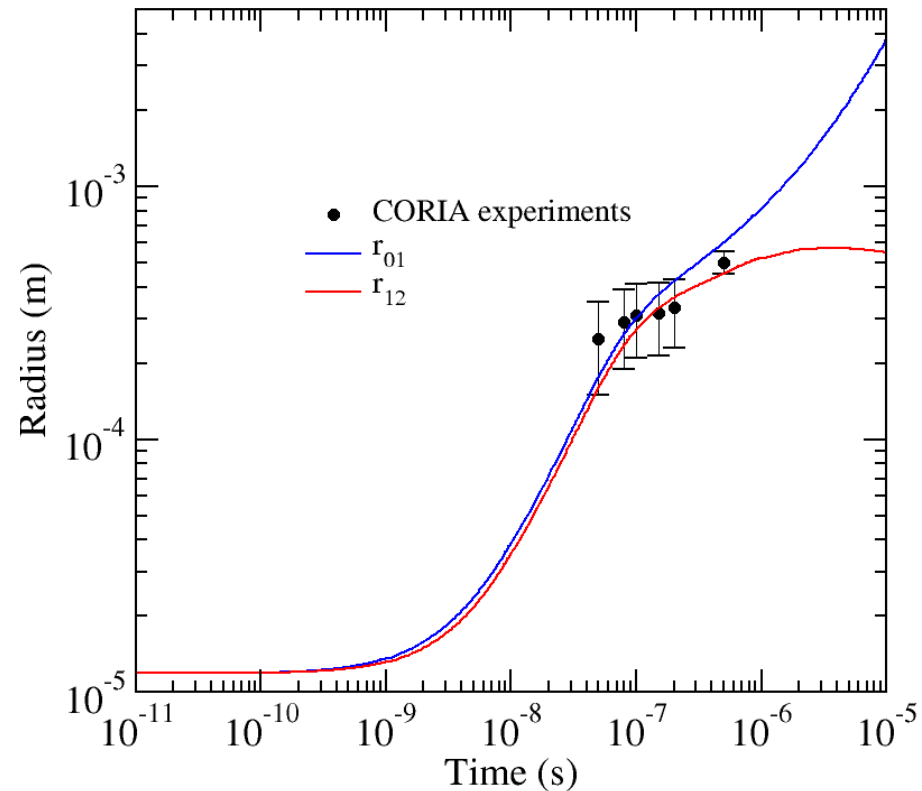
Plasma extinction for t ~ 500 ns

Temperature – Expansion

W (Ar, p_{atm}) 30 ps 532 nm 10 J cm^{-2}



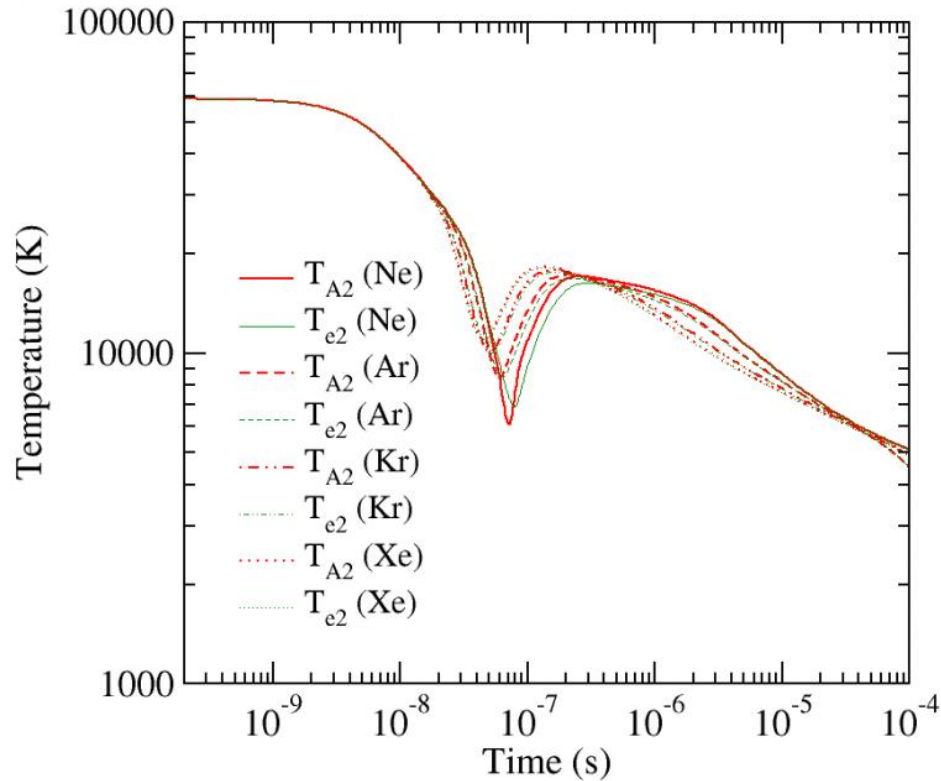
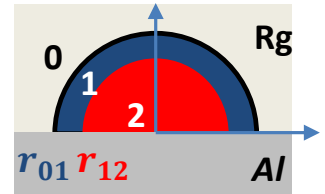
Calculated temperature slightly higher...



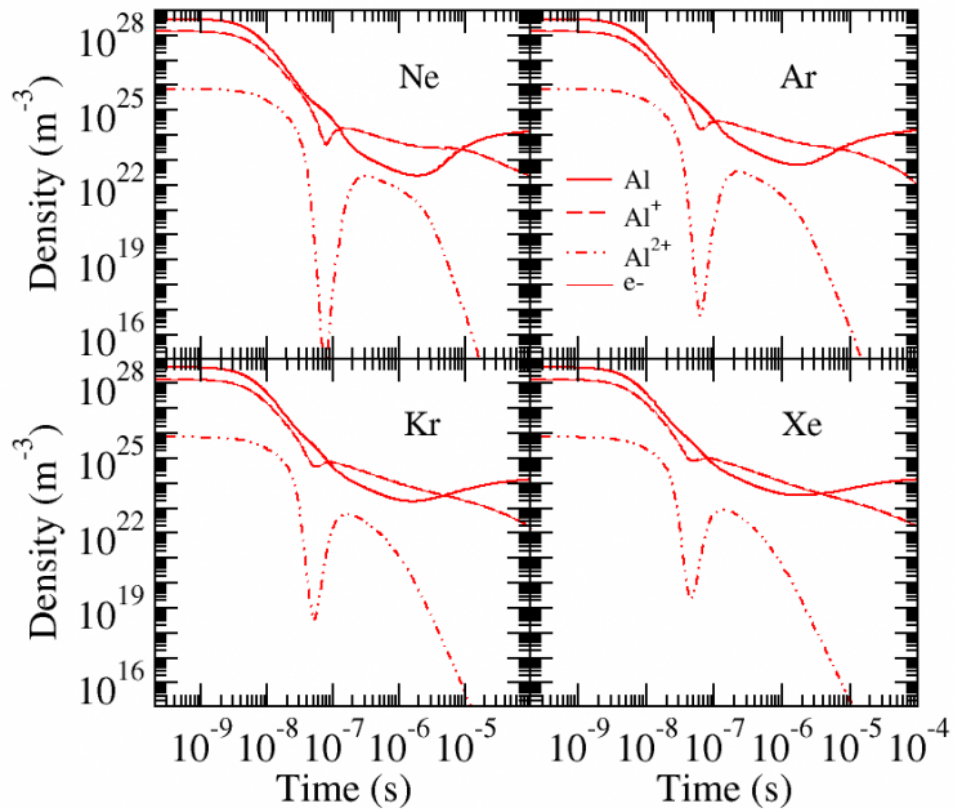
Satisfactory agreement for the radii...

Temperature - Chemistry

Al (p_{atm}) 10 ps 532 nm 10 J cm^{-2}



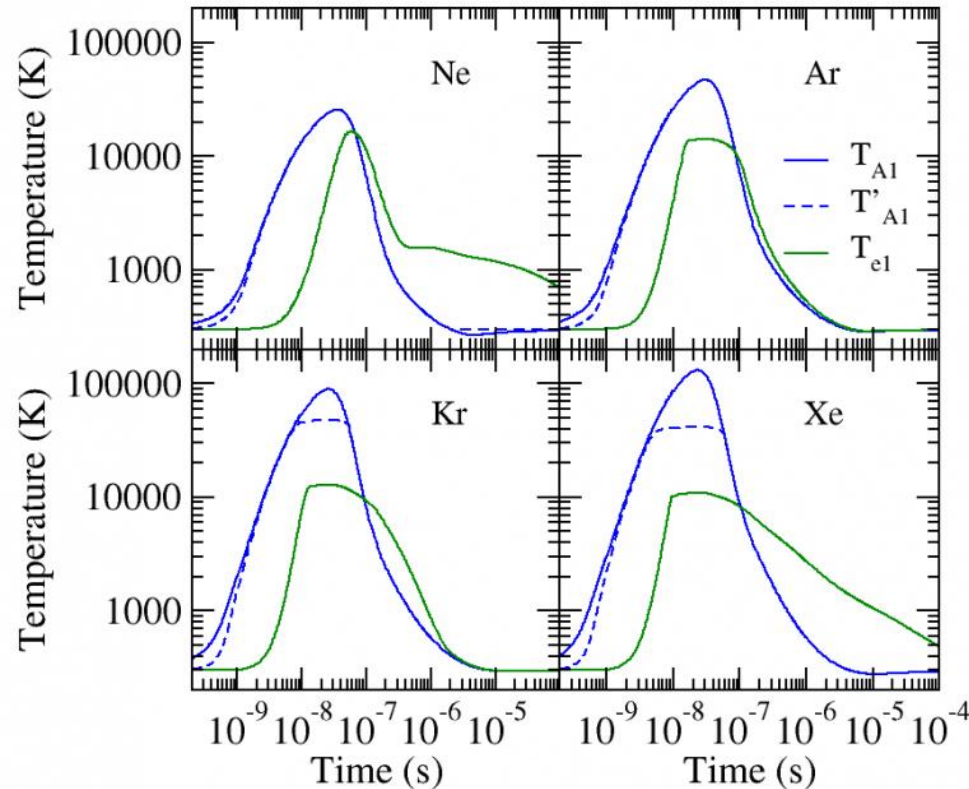
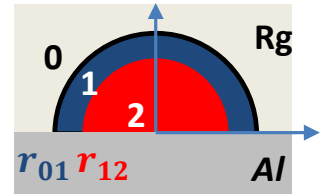
Strong decrease in T_A and $T_e \sim 70 \text{ ns}$ due to the pressure



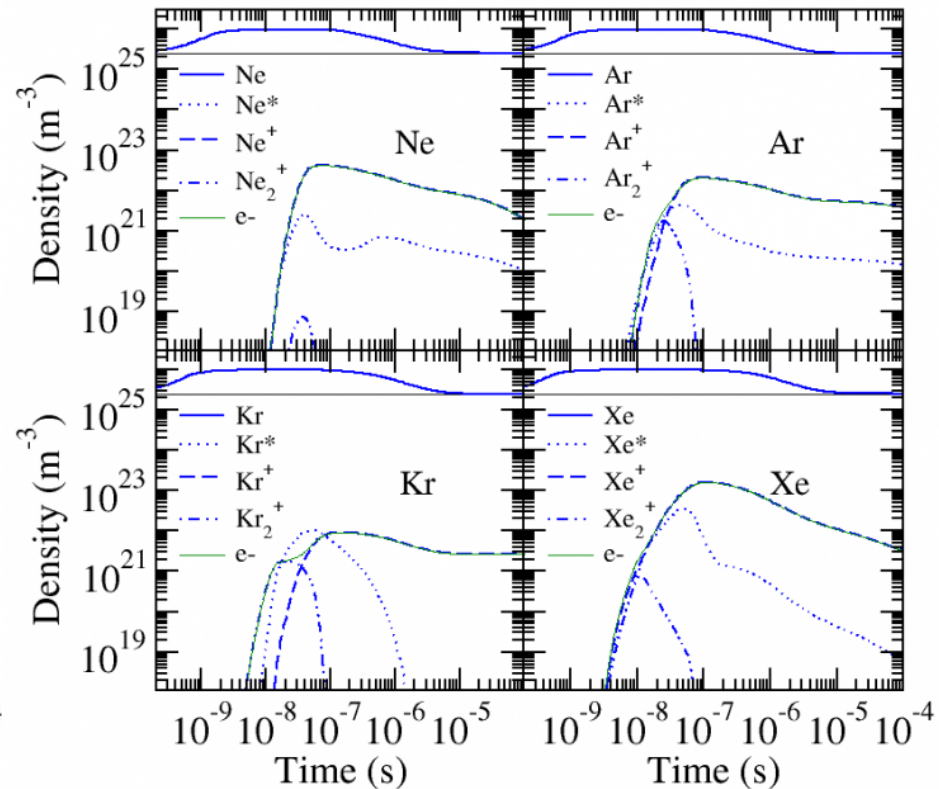
Strong decrease in $[\text{Al}^{2+}]$ for $\sim 70 \text{ ns}$ due to T

Shock layer

Al (p_{atm}) 10 ps 532 nm 10 J cm^{-2}



Strong thermal non equilibrium



Strong influence of Rg_2^+ at the beginning
Then replaced by that of Rg^+